

# Phased occupation and retreat of the last British–Irish Ice Sheet in the southern North Sea; geomorphic and seismostratigraphic evidence of a dynamic ice lobe

Dayton Dove<sup>1</sup>, David J.A. Evans<sup>2</sup>, Jonathan R. Lee<sup>3</sup>, David H. Roberts<sup>2</sup>, David R. Tappin,<sup>3</sup> Claire L. Mellett<sup>1</sup>, David Long<sup>1</sup>, S. Louise Callard<sup>2</sup>

<sup>1</sup>British Geological Survey, Lyell Centre, Edinburgh, EH14-4AP, UK

<sup>2</sup>Department of Geography, Durham University, Durham, DH1 3LE, UK

<sup>3</sup>British Geological Survey, Keyworth, Nottingham, NG12 -5GG, UK

1 **Phased occupation and retreat of the last British–Irish Ice Sheet in the**  
2 **southern North Sea; geomorphic and seismostratigraphic evidence of a**  
3 **dynamic ice lobe.**

4 Dove, Evans, Lee, Roberts, Tappin, Mellet, Long, Callard

5 *Keywords:*

6 Pleistocene glaciation, Last Glacial Maximum;

7 Deglaciation, Glaciology;

8 Northwest Europe, North Sea;

9 Bathymetry, Glacial geomorphology, seismic stratigraphy,

10 **Abstract**

11 Along the terrestrial margin of the southern North Sea, previous studies of the MIS 2 glaciation  
12 impacting eastern Britain have played a significant role in the development of principles relating to  
13 ice sheet dynamics (e.g. deformable beds), and the practice of reconstructing the style, timing, and  
14 spatial configuration of palaeo-ice sheets. These detailed terrestrially-based findings have however  
15 relied on observations made from only the outer edges of the former ice mass, as the North Sea  
16 Lobe (NSL) of the British-Irish Ice Sheet (BIIS) occupied an area that is now almost entirely submarine  
17 (c.21-15 ka). Compounded by the fact that marine-acquired data have been primarily of insufficient  
18 quality and density, the configuration and behaviour of the last BIIS in the southern North Sea  
19 remains surprisingly poorly constrained. .

20 This paper presents analysis of a new, integrated set of extensive seabed geomorphological and  
21 seismo-stratigraphic observations that both advances the principles developed previously onshore  
22 (e.g. multiple advance and retreat cycles), and provides a more detailed and accurate reconstruction  
23 of the BIIS at its southern-most extent in the North Sea. A new bathymetry compilation of the  
24 region reveals a series of broad sedimentary wedges and associated moraines that represent several  
25 terminal positions of the NSL. These former still-stand ice margins (1-4) are also found to relate to  
26 newly-identified architectural patterns (shallow stacked sedimentary wedges) in the region's seismic  
27 stratigraphy (previously mapped singularly as the Bolders Bank Formation). With ground-truthing  
28 constraint provided by sediment cores, these wedges are interpreted as sub-marginal till wedges,  
29 formed by complex subglacial accretionary processes that resulted in till thickening towards the  
30 former ice-sheet margins. The newly sub-divided shallow seismic stratigraphy (at least five units)  
31 also provides an indication of the relative event chronology of the NSL. While there is a general  
32 record of south-to-north retreat, seismic data also indicate episodes of ice-sheet re-advance  
33 suggestive of an oscillating margin (e.g. MIS 2 maximum not related to first incursion of ice into  
34 region). Demonstrating further landform interdependence, geographically-grouped sets of tunnel

35 valleys are shown to be genetically related to these individual ice margins, providing clear insight  
36 into how meltwater drainage was organised at the evolving termini of this dynamic ice lobe. The  
37 newly reconstructed offshore ice margins are found to be well correlated with previously observed  
38 terrestrial limits in Lincolnshire and E. Yorkshire (Holderness) (e.g. MIS 2 maximum and Withernsea  
39 Till). This reconstruction will hopefully provide a useful framework for studies targeting the climatic,  
40 mass-balance, and external glaciological factors (i.e. Fennoscandian Ice Sheet) that influenced late-  
41 stage advance and deglaciation, important for accurately characterising both modern and palaeo-ice  
42 sheets.

## 43 **1. Introduction**

44 The extent, pattern, and timing and dynamics of Late Devensian (Weichselian / Marine Isotope Stage  
45 (MIS) 2) glaciation in the southern North Sea has long been discussed, not least due to the classic  
46 terrestrial field sites located along the adjacent Norfolk, Lincolnshire, and eastern Yorkshire coasts  
47 (e.g. Catt & Penny 1966; Madgett and Catt, 1978; Pawley et al., 2006., Catt, 2007; Evans & Thomson,  
48 2010; Bateman et al. 2015), including the type site for the Last Glacial Maximum (LGM) within the  
49 British Isles at Dimlington (Penny et al. 1969; Rose, 1985; Bateman et al. 2011). Despite the  
50 abundance of onshore evidence, and conjectures on the offshore pattern/limits of glaciation  
51 (Valentin 1957; Eyles et al. 1994; Boston et al. 2010), the dynamics of North Sea glaciation remain  
52 poorly constrained due to the relative lack of detailed observations from the modern marine  
53 environment, even for the Late Devensian (Graham et al., 2011; Clark et al., 2012). Increasing the  
54 evidence-base and our understanding of the offshore glacial geology will therefore: i) better  
55 constrain the regional history and behaviour of the former British-Irish Ice Sheet (BIIS) in the North  
56 Sea and its relationship with the Fennoscandian Ice Sheet (FIS); and ii) provide insight into the  
57 dynamics of recession of a major ice lobe during deglaciation. The latter has important implications  
58 for the potential collapse of contemporary ice lobes in response to future climate change.

59 Similar to many other mid and high-latitude regions, much of our current knowledge of the dynamics  
60 of glaciation within the North Sea basin has been inferred from neighbouring terrestrial sequences in  
61 the UK (Eyles et al. 1994; Evans et al., 1995; Catt 2007; Boston et al., 2010; Evans & Thomson 2010;  
62 Clark et al., 2012; Bateman et al., 2015; Busfield et al., 2015) and continental Europe ([Houmark-  
63 Nielsen, 2007, 2011; Laban & van der Meer, 2011; Böse et al., 2012](#)). Marine-acquired information  
64 only provides the basis for a crude model of the long-term glacial evolution of the southern North  
65 Sea (e.g. Veenstra et al., 1965; Cameron et al., 1987; Ehlers et al., 1984; Balson and Jeffrey, 1991;  
66 Laban, 1995; Sejrup et al., 2000; [Laban & van der Meer, 2011](#); Lee et al., 2011). Furthermore, the  
67 relative lack of marine data has resulted in a range of disparate spatial reconstructions for specific

68 periods of glaciation, in particular the mid to late Devensian (Carr et al., 2006; Sejrup et al., 2009;  
69 Graham et al., 2011) (Fig. 1).

70 To address these contrasting interpretations this paper presents a series of new marine  
71 observations, which in combination with terrestrial evidence, enables an enhanced model for the  
72 occupation and retreat of the BISS in the southern North Sea. We utilise an extensive new  
73 compilation of bathymetry data together with legacy 2D seismic data to constrain the pattern, style,  
74 and relative chronology of glaciation during the last glacial cycle. Linkages are drawn between  
75 seabed geomorphology and seismic stratigraphy to provide a more detailed model of the offshore  
76 glacial geology. Until now, regional bathymetry data have not been of sufficient resolution to  
77 identify and describe glacial landforms and landform assemblages, and the area's legacy seismic data  
78 have not been exploited to investigate the regional-scale glacial stratigraphy. The updated model  
79 enables an improved correlation between marine and terrestrial glacial features associated with  
80 the North Sea lobe of the BISS.

## 81 **Location and Bathymetry**

82 The study area lies in the southern North Sea, bordered by the East Yorkshire (Holderness) and  
83 Lincolnshire coasts to the west, and the Norfolk coast to the south (Figs. 1, 2). Bathymetry data  
84 records a number of features unrelated to past glacial processes, including mobile sediment  
85 bedforms associated with the Holocene marine transgression and modern hydrodynamic processes,  
86 as well as exposed pre-Quaternary bedrock (e.g. Tappin et al., 2011). Sedimentary bedforms of  
87 marine (current-induced) origin are ubiquitous at seabed across the study area and include large-  
88 scale sediment banks (up to 40m in height), sediment waves (up to 10 m in height), fields of small  
89 sand waves (megaripples), as well as sand ribbons, patches, and sheets (e.g. Tappin et al., 2011)  
90 (Figs. 2,3,4). Quaternary sediments are relatively thin and bedrock is commonly present within c.20  
91 m of the seabed (Harrison, 1992; Cameron et al., 1992). Within seabed-incised deeps, Quaternary  
92 sediments are commonly absent revealing bedrock composed of folded Cretaceous-age Chalk (Inner  
93 Silver Pit) (Fig. 3), and Jurassic/Triassic sand- and mudstones (Sole Pit) (Donovan, 1972; Cameron et  
94 al., 1992; Tappin et al., 2011; [Mortimore & James, 2015](#)). A broad and elongated channel-system  
95 extends from the Inner Silver Pit southwards towards the Wash in-which Cretaceous (Chalk) and  
96 Jurassic (mudstone) bedrock crop-out ([Gallois, 1994](#)).

## 97 **Glacial history of the study area**

98 Much of our current understanding of the shallow geology of the southern North Sea originates from  
99 analysis and interpretation of data acquired during a systematic British Geological Survey (BGS  
100 programme of offshore geophysical surveying and ground-truthing ) between the late 1970's and  
101 early 1990's (Long et al., 1988; Fannin, 1989; BGS, 1991; Cameron et al., 1992). Supported by the

102 existing, but sparse literature (e.g. Jansen et al., 1979), this survey activity led to the establishment  
103 of a coherent regional seismostratigraphic framework calibrated from shallow cores and boreholes  
104 (Stoker et al., 2011). The glacial component of the Quaternary succession has conventionally been  
105 partitioned into three glacial stages (separated by interglacial marine deposits) and, based upon  
106 correlation with the Dutch succession, ascribed to the following stages of glaciation: MIS 12  
107 (Anglian/Elsterian), MIS 10-6 (Saalian), and MIS 5d-2 (Devensian/Weichselian) (Cameron et al., 1987;  
108 Balson and Jeffrey, 1991; Laban, 1995). However, recent work has indicated additional stages of  
109 glaciation both pre- and post-dating the Middle Pleistocene (Ekman, 1998; Carr et al., 2006; Graham  
110 et al., 2011; Lee et al., 2011, 2016; Dowdeswell & Ottesen, 2013). Farther north, at least 7 stages of  
111 glaciation have been proposed using multiple generations of cross-cutting tunnel valleys observed in  
112 3D seismic data (e.g. Stewart and Lonergan 2011). This increased sub-division of glacial episodes in  
113 the Quaternary has become broadly accepted, and looks increasingly tenable given the time-  
114 transgressive behaviour of the BIIS and the neighbouring FIS during the late glacial stage (c.32-11.5  
115 ka) (Scourse et al., 2009; Böse et al., 2012; Kalm, 2012; Hughes et al., 2016). The emerging picture  
116 from both empirical reconstructions and model results is of a highly-dynamic last BIIS, exhibiting  
117 complex behaviour through binge-purge cycles, migrating ice divides and flow regimes, as well as  
118 interaction with the neighbouring FIS (Hubbard et al., 2009; Clark et al., 2012; Livingstone et al.  
119 2012).

120 The maximum extent of the last BIIS within the North Sea has been depicted in a wide range of  
121 reconstructions (Fig.1; Graham et al., 2011 and references therein). Carr et al. (2006), building upon  
122 the work of Sejrup et al. (1994; 2000), provides the most detailed account of Late Devensian North  
123 Sea glaciation, based on micromorphological analysis of tills combined with seismostratigraphy.  
124 They propose several phases of Devensian glaciation with two early episodes ('Ferder' c.70 ka; 'Cape  
125 Shore' c.29-20 ka) involving confluence of the BIIS and FIS in the North Sea, but not extending  
126 farther south than Holderness (Figs. 1, 2). During a final re-advance, termed the 'Bolders Bank  
127 Episode', ice extended southwards down the western side of the North Sea Basin between c.18-  
128 16kya, with the BIIS uncoupled from the FIS. The presence of this 'North Sea Lobe' (NSL) was  
129 originally inferred from the recovery of glacial deposits (Bolders Bank Formation) within the  
130 southern North Sea (e.g. Jansen et al., 1979; Balson and Jeffrey, 1991), and although discounted by  
131 some early ice sheet models of the BIIS (e.g. Boulton et al., 1977), ice sheet lobes such as the NSL are  
132 now understood to represent characteristic, if ephemeral, components of the palaeo-ice sheet  
133 system (e.g. Boulton and Hagdorn, 2006; Hubbard et al., 2009).

134 The interaction with the FIS is particularly important for understanding the behaviour of the BIIS  
135 within the North Sea, and while this has not always been the case, it is now broadly accepted that

136 the BIIS and FIS were coalescent within the North Sea basin at some point(s) during the mid-late  
137 Devensian (Boulton et al., 1985; Sejrup et al., 1994, 2009; Carr et al., 2006; Bradwell et al., 2008).  
138 While this coalescence likely peaked during the maximum extent of ice sheets (BIIS at ~c.29-23 ka -  
139 e.g. Scourse et al., 2009), the time-varying confluence with the FIS may have also influenced the flow  
140 configuration of the NSL within the western North Sea. While Carr et al. (2006) did not invoke BIIS-  
141 FIS coalescence during this most recent glacial episode, the southerly flow trajectory of the NSL is  
142 more difficult to reconcile without some buttressing effect by the FIS (e.g. Graham et al., 2011;  
143 Busfield et al., 2015; Sejrup et al., 2016).

144 Accounting for the uncertainty in MIS 2 ice sheet reconstructions for the region, Clark et al. (2012)  
145 present two end-member reconstructions for the North Sea and east coast of Britain: 1) early  
146 (~27kya) and complete breakup of North Sea Ice with a later surge lobe into the southern North Sea  
147 and along the east coast at ~17kya; 2) persistent ice in the southern North Sea from 27 kya, with a  
148 re-advance farther south from ~19-17kya. Both Carr et al. (2006) and Clark et al. (2012) acknowledge  
149 that the maximum southern extent of the BIIS within the North Sea may not correspond to its  
150 maximum eastern advance. The primary observations conventionally used (though not always  
151 attributed) to define the LGM limit within the southern North Sea (and within this study area) are: 1)  
152 the extent of the Bolders Bank Formation (BGS, 1991), and 2) the southern limit of several incised  
153 deeps which are interpreted as glacial tunnel valleys (Ehlers and Wingfield, 1991). The tunnel valleys  
154 are common in the North Sea, and attributed to a number of discrete glacial episodes (Stewart and  
155 Lonergan, 2011; Van der Vegt et al., 2012). Those attributed to the Elsterian (MIS 12) are usually  
156 larger, and extend farther south than those attributed to the Weichselian/Devensian (MIS 2) (Huuse  
157 and Lykke-Anderson, 2000). Some of the MIS 2 tunnel valleys within this southern North Sea study  
158 area remain exposed at seabed whereas others have been infilled with post-glacial sediment  
159 (Wingfield, 1990; Praeg, 2003; Tappin et al., 2011; Moreau and Huuse, 2014).

160 Deposits relating to Late Devensian glaciation within the southern North Sea, and attributed to the  
161 NSL, are represented by the Bolders Bank Formation (BBF). First described by Veenstra (1965) in the  
162 area surrounding the Outer Silver Pit (Fig. 2), the BBF as a seismostratigraphic unit was subsequently  
163 mapped across the region by the BGS (e.g. BGS, 1991). In the south the formation extends to near  
164 the North Norfolk coast at c.53° N, and in the north to c.55°N, where it is considered laterally-  
165 contiguous with the Wee Bankie Formation (Fig. 1) (Gatliff et al., 1994; Davies et al., 2011).

166 Sediment cores reveal that while variable, the BBF commonly comprises dense reddish-brown (or  
167 grey-brown) fine-grained diamicton, with sub-rounded to sub-angular clasts. Shallow seismic data  
168 show that the unit is c.5-20 m thick, acoustically homogenous, and exhibits a prominent generally  
169 flat basal reflector indicative of extensive erosion. The BBF is interpreted as a subglacial till

170 (Cameron et al., 1987; Carr, 1999; Davies et al., 2011). Clast petrology together with heavy mineral  
171 and derived palynomorphs suggest provenance from the Grampian Highlands and the Midland  
172 Valley of Scotland, northern England, and the margins of the western North Sea (Carr et al., 2006;  
173 Davies et al., 2011). At its eastern margin, the BBF has previously been thought to interdigitate with  
174 the Dogger Bank Formation (Cameron et al., 1992), though this relationship is being revised  
175 following recent research on Dogger Bank (Cotterill et al., in review).

176 The BBF comprises at least two distinct acoustic members separated by unconformities (e.g.  
177 Harrison, 1992), however the reason for this subdivision is not known and has not previously been  
178 investigated (i.e. process/origin of distinct members). Despite this knowledge gap, it has long been  
179 suggested that the BBF resembles, and is correlative with adjacent till sequences attributed to the  
180 Dimlington Stadial in East Yorkshire (Catt, 2007; Evans & Thomson, 2010; Roberts et al., 2013),  
181 Lincolnshire, and north Norfolk (Madgett and Catt, 1978; Cameron et al., 1992; England and Lee,  
182 1991). Confined to a narrow belt along the coastal margin (Fig. 1), these sequences relate to the  
183 maximum onshore extent of the NSL and record complex patterns of ice marginal processes and  
184 dynamics (Evans et al., 1995; Pawley et al., 2006; Moorlock et al., 2008; Evans & Thomson 2010;  
185 Boston et al., 2010; Roberts et al., 2013). Recently published OSL dates indicate that the maximum  
186 onshore extent of the NSL in East Yorkshire was reached between 21-18 ka BP (Bateman et al.,  
187 2015), which is broadly comparable with the tentatively inferred age of the BBF (Carr et al., 2006). It  
188 is also worth noting that a large proglacial lake within the southern North Sea has been inferred by  
189 some researchers (e.g. Clark et al., 2012), pooled between the coalescent BIIS and FIS to the north  
190 and a shallow sill across the English Channel. While such a regional-scale lake appears  
191 topographically feasible, in situ data have yet to support this hypothesis.

192

193 The mapped occurrence of the BBF (constraining the maximum offshore extent of NSL) together  
194 with high-fidelity onshore stratigraphies provides an indication that the NSL was a dynamic  
195 component of the BIIS, extending down the western North Sea during the last glacial cycle (Jansen et  
196 al., 1979; Stokes and Clark, 2001; Carr et al., 2006; Graham et al., 2011). It is hypothesized that the  
197 NSL oscillated over time to produce the multiple tills and intervening stratified sediments that are  
198 now observed onshore (e.g. Evans and Thompson, 2010; Roberts et al., 2013), as well as impounded  
199 large proglacial lakes in the unglaciated Vale of Pickering (Kendall 1902; Evans et al. 2016),  
200 deglaciated Tees (Agar 1954; Plater et al. 2000), Wear (Smith 1981, 1994; Teasdale & Hughes 1999)  
201 and Vale of York (Bateman et al. 2008, 2015; Fairburn & Bateman 2015). Apart however from the  
202 first-order mapping of the BBF, these studies are almost entirely reliant on evidence from a narrow  
203 belt along the reconstructed NSL margins (Figs.1,2), leaving significant potential for improved

204 characterisation of the process-form regime responsible for BBF emplacement within the former NSL  
205 trunk zone, up-ice from the ice sheet termini. This evidence must necessarily come from the  
206 offshore environment where the full transition from the subglacial environment through to the  
207 deglacial terrain can be investigated, and in which potential features relating to the dynamic glacial  
208 evolution of the region may be placed in a robust stratigraphic and relative chronological  
209 framework.

## 210 **2. Methodology**

211 This study involved the integrated interpretation of bathymetry, shallow seismic, and sediment core  
212 data from various sources over a large study area (c.25,000 km<sup>2</sup>) extending to 003° E in the east, and  
213 c.54° N in the north (Fig. 1). The study area is similar to that covered by the Humber Regional  
214 Environmental Characterisation (REC) report by Tappin et al. (2011), but has been expanded to  
215 incorporate further features of interest. It was in fact tentative, though un-reported observations  
216 (e.g. origin of regional bathymetric high and potential relationship with tunnel valleys) of a lower-  
217 resolution bathymetry dataset made during that work that inspired this more focussed glacial study.

### 218 **2.1 Bathymetry**

219 Existing bathymetry data have been compiled and re-gridded to produce a single bathymetric  
220 surface for geomorphological interpretation. The collated data were taken from multiple sources of  
221 varying age (late 1970's - late 2000's), lineage, and resolution (e.g. singlebeam vs multibeam swath  
222 bathymetry) to form a Digital Elevation Model (DEM) at 25 m horizontal resolution. Underlying  
223 datasets are open access and may be downloaded from the UK bathymetry Data Archive Centre  
224 (DAC) website. Applying glacial geomorphological principles that were originally developed in  
225 terrestrial settings to the submarine environment has become increasingly possible from the  
226 extensive bathymetric datasets now available (e.g. Todd et al., 2007; Bradwell et al., 2008; Dove et  
227 al., 2015). This approach is particularly applicable to the British Isles as it has been estimated that  
228 two-thirds of the BIIS (MIS 2) was situated in what is currently a submerged marine environment  
229 (Clark et al., 2012).

230 Approximately 10% of the area has been mapped using high-resolution (1-5 m) swath bathymetry,  
231 and these data have been incorporated into the 25 m bathymetric surface. These bathymetry  
232 datasets are mainly distributed along the coasts, as well as extending from the Humber Estuary to  
233 around the Inner Silver Pit (Figs. 2,). Where swath bathymetry data are not available, we rely upon  
234 older (1979-2005) single-beam echo-sounder data. These survey lines are sufficiently dense to  
235 support the regional 25m resolution bathymetry surface, but in a few places are spaced greater than  
236 25 m and thus we have over-sampled the underlying data. While multiple smaller features (e.g.

237 sediment waves and ribbons) can only be adequately observed on the swath bathymetry data, the  
238 glacial features of interest in this study are well imaged at 25m resolution (Figs. 4,5).

## 239 2.2 Seismic

240 The shallow sub-seabed geology has been interpreted from digital scans of single-channel seismic  
241 data acquired by the BGS as part of the regional mapping programme from between the late 1970's  
242 and early 1990's (Fannin, 1989), as well as from a Regional Environmental Characterization (REC)  
243 funded by the Aggregates Levy (Tappin et al., 2011). There are significant volumes of 2D seismic  
244 (pinger, boomer, sparker, airgun) data of variable quality available in the region. Principally, the  
245 surface-towed boomer data from 1990/4, 1993/1, and 2008/5 surveys are most useful. Quaternary  
246 maps based on these data resulted in the published 1:250k maps of Spurn (e.g. BGS, 1991). The  
247 commissioned aggregates study, Harrison (1992), also provides a useful cross-reference for our  
248 seismic interpretations. Using the available seismic data in the region, we have developed a new  
249 (glacial) seismostratigraphic framework to more accurately characterise the sub-surface data  
250 (seismic and sediment cores) and its relationship to the glacial geomorphological features preserved  
251 at seabed. While we have examined a large proportion of the available data to confirm the validity  
252 of our interpretations, we have not systematically re-mapped the shallow geology of the region.  
253 Instead we present several representative profiles to demonstrate the revised seismic stratigraphy  
254 (Figs. 6-8). One final consideration is the navigational accuracy of data acquired prior to the use of  
255 Global Positioning System (GPS) in the mid 1990's. Data acquired prior to the mid 1980's were based  
256 on the Decca Navigator Main chain with accuracies of approximately  $\pm 100$  m. From the mid 1980's  
257 through to the use of GPS, accuracies were nearer  $\pm 10$  m using the Sydelis positioning system.  
258 Although it is important to acknowledge this navigational uncertainty in order to avoid over-  
259 interpreting correlations with seabed features, the landforms of interest in this study are sufficiently  
260 large (100's metres - kilometre scale) that such problems are effectively negligible.

## 261 2.3 Sediment cores

262 BGS-held sediment core records were used to cross-reference interpretation of the seismic data.  
263 While no new core analysis or re-interpretation was undertaken, existing core descriptions and  
264 classifications were used to validate our geomorphic and seismostratigraphic interpretations.  
265 Approximately 1800 sedimentary cores are distributed throughout the study area, 400 of which  
266 include sediment previously interpreted at subglacial till. Vibrocoreing was the most common  
267 equipment type used in the region, although gravity and rock corers were also used (e.g. Fannin,  
268 1989).

## 269 3. Results

### 270 3.1 Seabed Geomorphology

271 The large-scale morphology of the seabed is characterized by a broad, arcuate, low-relief  
272 bathymetric high extending eastwards from the Holderness and Lincolnshire coasts and a series of  
273 large valleys incised approximately perpendicularly into this high (Fig. 2). Water depths generally  
274 increase eastward away from the Lincolnshire coast, but also north and south of the regional  
275 bathymetric high. Over the high, water depths are commonly ~15 m in the west, increasing to 20-30  
276 m in the east. Water depths over the coastal platforms (shallow bedrock and/or tidal flats) and  
277 within The Wash, are very shallow at <10 m. For example, water depths of less than 5 m extend  
278 nearly 20 km north of the Norfolk coast on the Burnham Flats (Fig. 2). The deepest parts of the study  
279 area are found within the incised deeps, with water depths reaching nearly 100 m in the Inner Silver  
280 Pit. Results sections 3.1 - 3.3 describe the physical characteristics of several glacial features observed  
281 in the bathymetry (Section 3.1), sediment core (3.2), and shallow seismic stratigraphy (3.3) data. An  
282 interpretation of these glacial features is given in section 3.4, based on the integration of  
283 observations and analysis of the three data types.

#### 284 3.1.1 Arcuate ridge complexes

##### 285 **Regional bathymetric high and broad sediment wedges (BBSWs)**

286 The regional bathymetric high extends c.170 km eastward from the Holderness and Lincolnshire  
287 coasts towards Dogger Bank with a variable width up to 90 km (Figs. 2,4). It is arcuate in plan-view,  
288 oriented NW-SE adjacent to Holderness in the west, turning SW-NE in the east. The high comprises  
289 several smaller bathymetric highs, hereby called broad sediment wedges (BBSW), which are also  
290 elongate and arcuate in plan-view. These features range in width from approximately 10-25 km, are  
291 approximately 10-20 m in height. They exhibit a broad wedge-like morphology in cross-section (i.e.  
292 subtle changes in vertical relief over large geographic areas), with relatively steep-dipping  
293 southward-facing margins and gently-dipping northward slopes (Figs. 2,4). South-dipping slopes  
294 descend locally into shallow, elongate depressions that separate the broad sediment wedges. Apart  
295 from the more-pronounced southern margins, the boundaries of the sediment wedges are generally  
296 diffuse and irregular, becoming particularly difficult to identify in the west where coastal  
297 sedimentation and mobile sediment bedforms progressively obscure their seabed expression.

##### 298 **Narrow Ridges (NR)**

299 Narrow ridges, c.500 m – 2 km wide, commonly delineate the southern terminus of the BSWs  
300 described above (Fig. 4) forming a series of discontinuous ridge-chains across the study area.  
301 Individual ridges exhibit a sinuous to saw-tooth plan-view morphology, are up to 10 m in height  
302 (though more commonly 1-2 m). They are frequently interrupted at seabed by other geomorphic

303 features such as Holocene sediment bedforms and the incised deeps. They exhibit no consistent  
304 asymmetry, but rest on the southern edge of the BSWs such that bathymetric relief on the southern  
305 slopes of the ridges is often greater where descending into the shallow depressions. Defining a  
306 distinct northern edge is often difficult as the ridges appear morphologically contiguous with the  
307 underlying BSWs.

308 The mapped location of the NRs is shown in Fig. 9, which collectively form four separate ridge-  
309 chains, ordered NR1-4 from south to north. The two northerly ridges (NR3 and NR4) are more  
310 distinctive and continuous than NR1 and NR2 which are more diffuse. A notable characteristic of  
311 NR3 is that several isolated loop-shaped (convex southward) ridge elements occur situated to the  
312 south of the main ridge (Fig. 4).

### 313 **3.1.2 Incised deeps**

314 Across the study area several large deeps (ID) are incised into the seabed and are up to 100m deep  
315 (c.80m below surrounding seabed), 45km length and 5km width (Fig. 2). The most prominent deeps,  
316 the Inner Silver Pit and Sole Pit, are eroded into bedrock. Several of these deeps are depicted within  
317 the seabed bathymetry whilst others can be recognised within shallow seismic data (Cameron et al.,  
318 1992; Tappin et al., 2011). All of the incised deeps exhibit U-shaped cross-sectional profiles and  
319 scoop-shaped longitudinal profiles with reverse slopes at both the northern and southern ends (Figs.  
320 2,3). In plan-view the incised deeps are linear-to-curvilinear in shape.

321 The orientation of these deeps is roughly perpendicular to the local orientation of the BSW into-  
322 which they are incised. As such, incised valleys radiate to the south fanning out to the west and east  
323 (Fig). The northern and southern rims of the incised deeps are broadly coincident with the  
324 respective northern and southern margins of the BSWs, though it is notable that the deeps  
325 commonly extend a further 2-5 km south of the BSWs, and the NRs that delimit their southern  
326 margin. For example, the Inner Silver and Sole Pits are incised into the northern-most BSW, with  
327 their southern rims extending just beyond NR4. This apparent landform association is repeated and  
328 clear for the northerly two BSWs (NR3 & 4), and potentially for the more subtle BSW associated with  
329 NR2. The narrow ridges also commonly turn northwards as they near the incised deeps (Figs. 2, 4).

### 330 **3.1.3 Coast-parallel offshore ridges**

331 Observed along ~50km of the Holderness coast, and extending up to ~20km offshore, we observe a  
332 large number of sharp-relief, thin ridges (commonly 100-150 m wide, 1-3 m high) which are oriented  
333 ~parallel to the adjacent coast (Fig. 5). Due to the small height and width of these features, they  
334 have primarily been mapped from high-resolution swath bathymetry data from just offshore,  
335 although they are coarsely visible on the 25m DEM where swath bathymetry data are not available.  
336 Individual ridges are commonly spaced ~500m apart, and although on a regional scale discontinuous,  
337 there are single continuous ridge lengths of up to ~8km. At the kilometre-scale the ridges are linear

338 to curvilinear in plan-view, but at a higher-resolution are seen to be zig-zag to sinuous. The ridges  
339 typically are asymmetric, with the steeper western-facing scarp slopes of up to 25°. The orientation  
340 of the offshore ridges broadly parallels the coast as well as the moraine ridges on Holderness (Fig.  
341 10a) (Evans & Thomson, 2010), although there is some variation in the orientation of separate  
342 groupings of ridges (NW-WE switching to NNW-SSE in northeast corner of Fig. (5)). These divergent  
343 orientation groups also appear to be pre-disposed by an underlying geomorphic fabric.

### 344 **3.2 Sediment Cores**

345 Where Holocene mobile sediments are thin, shallow cores located on the BSWs sample firm-to-stiff  
346 diamicton, interpreted as a subglacial till and attributed to the Bolders Bank Formation (BBF) (Figs.  
347 9,10) (Veenstra, 1965; Long et al., 1988, BGS 1991; Carr et al., 1999; Davies et al., 2011). The core  
348 samples reveal a clear boundary extending ENE from North Norfolk with till recovered in cores north  
349 of this boundary. This apparent boundary (together with seismostratigraphic observations) was  
350 previously used to map the regional extent of the BBF (BGS, 1991). This till limit (i.e. extent of BBF)  
351 also corresponds to the southern margin of the regional bathymetric high and its BSWs, suggesting a  
352 relationship between the BBF and the bathymetric relief of the region.

353 Few cores are located on the NRs (1-4), although where significant penetration (>50 cm) was  
354 achieved, till (i.e. BBF) was recovered. As a note however, this is one circumstance in the study  
355 where the navigational uncertainty (~10-100m) associated with legacy core records may lead to  
356 interpretation errors, especially as the NRs themselves are only ~500m – 2 km wide. Because of this  
357 uncertainty, the lithological interpretation of the NRs remains tentative. The BBF has previously  
358 been described as an overconsolidated reddish-brown (or grey-brown) fine-grained matrix-  
359 supported diamicton with sub-rounded to sub-angular clasts of local and far-travelled provenance  
360 (e.g. BGS, 1991; Carr et al., 1999, Davies et al., 2011), and this is confirmed by a preliminary review  
361 of legacy core records. A webGIS of the BGS-held sedimentary cores and scans of core description  
362 sheets can be found here: [http://mapapps2.bgs.ac.uk/geoindex\\_offshore/home.html](http://mapapps2.bgs.ac.uk/geoindex_offshore/home.html).

### 363 **3.3 Seismic Stratigraphy –shallow stacked till complex**

364 Within this section shallow seismic data are investigated to establish links between the shallow  
365 seismic stratigraphy and the geomorphic observations presented above. Several representative  
366 cross-sectional profiles (A-A' – Fig. 6; B-B' – Fig. 7; C-C' – Fig. 8) are presented which are orientated  
367 broadly perpendicular to the observed seabed geomorphic trends. While these cross-sections  
368 cannot capture every detail and stratigraphic variation that occurs in the area, they portray the  
369 common architectural trends which are consistently observed across the area. It is also worth  
370 emphasizing that like the seabed geomorphological record, subtle vertical relief is spread across

371 large geographic distances (10's kms), thus the data examples and cross-sections are presented with  
372 significant vertical exaggeration to clearly demonstrate the stratigraphic relationships.

373 **Profile A-A'** presents a long (57 km) interpreted profile (Fig. 6a) and subset data example (Fig. 6b)  
374 from a BGS boomer survey (1990/4 - 1). It serves as our 'type-section', and is broadly representative  
375 of the Quaternary succession within the study area (Fig 2). This N-S oriented profile crosses the  
376 northerly-most BSW and NR4, as well as NR3 that converges on NR4 in this location. Further south,  
377 profile A-A' partly crosses the BSW associated with NR2 (Fig. 9). There are several Holocene features  
378 (mobile sediment-wave fields, prominent sediment bank) that partially obscure the glacial record  
379 causing attenuation of the acoustic signal, thereby masking the underlying stratigraphy, and partially  
380 inhibiting a continuous interpretation north and south of the bank (Fig. 6). There are also several  
381 shallow channels which are eroded into the seabed and interpreted as Holocene channels formed by  
382 fluvial incision prior to marine transgression (Fitch et al., 2005; Gaffney et al., 2007)). Pre-MIS 2  
383 stratigraphic units are also present in the form of Egmond Ground (light brown) and Sand Hole (dark  
384 brown) formations, both inferred as interglacial (Holstenian/Hoxnian) deposits (BGS, 1991; Harrison,  
385 1992; Cameron et al., 1992).

386 While the BBF was previously mapped as a single seismic unit across the region (e.g. BGS, 1991;  
387 Harrison, 1992), here we provide evidence that the BBF can be subdivided into multiple  
388 seismostratigraphic units (SU), separated by unconformities. Where the BBF SUs outcrop at/near  
389 seabed, sediment-core data indicate they comprise till previously interpreted as BBF (undivided)  
390 (Fig. 9). Along profile A-A' we observe five clear SUs that are shallowly and progressively stacked  
391 (predominantly) from south to north, younging northwards. In other words, BBF tills outcropping  
392 at/near seabed in the south are mostly stratigraphically deeper and older than those farther to the  
393 north. The acoustic character of the five SUs is typically homogenous/massive with few internal  
394 laterally-continuous reflectors, with only isolated examples of conformable/bedded stratigraphy.  
395 Acoustic reflectors separating 5 SUs are high-amplitude and are typically planar where the  
396 underlying SU is not topography-forming (e.g. ridge). Four or five generations of channels (defined  
397 by stratal position and cross-cutting relationships) can be identified which are eroded into and below  
398 these stacked BBF SUs along A-A'. As with the SUs themselves, the channels observed in the south  
399 occur at lower stratal levels than those observed farther north, indicating that the southerly buried  
400 channels are predominantly older than those in the north, which include the northern tip of a  
401 seabed incised deep (Figs. 6,9).

402 Before describing the SUs (I-V) observed along profile A-A' in detail, it is important to note that  
403 acoustic character alone cannot be used to discriminate between SUs (e.g. correlating across broad  
404 lateral distances), as they don't exhibit uniquely identifiable characteristics. This may be due to the

405 age and quality of the data, and/or the variability of the physical properties of the remotely-sensed  
406 sediment. Across the region, the BBF exhibits stratigraphic variability and local-scale complexity, and  
407 for this reason we do not assume that each of SUs I-V observed on profile A-A' can be individually  
408 traced across the study area. Instead, what usefully characterises the SUs (and where pattern can be  
409 found) is the aggregated stratal architecture of the BBF across broader scales (>10-20 km), and as  
410 we'll shortly describe, their association with seabed geomorphological features. Despite that  
411 individual BBF SUs variably exhibit irregular, to tabular, to buried-ridge morphologies (Fig. 2), the  
412 combined stack of BBF SUs consistently form low-relief wedges along regional cross-sectional  
413 profiles oriented perpendicularly to the arcuate ~E-W bathymetric trends. These broad wedges are  
414 relatively thicker and more acutely tapered/pinched-out towards their southern limit (e.g. Fig. 6).

### 415 3.3.1 Seismostratigraphic Units (SUs) – Profiles A-A' and B-B'

416 Five seismic units (SUs) are observed along our type-section, profile A-A' (Fig. 6). The shorter profile  
417 B-B' presents a portion of BGS seismic line 1990/4 -21 approximately 9 km east of profile A-A' (Fig.  
418 7), and is included here to reveal the southern projection of structures (i.e. buried wedge)  
419 comprising SUs I & II which are truncated at the southern end of profile A-A' (Figs. 2, 9).

420 The stratigraphically deepest **SU I** is observed along the southern portion of profile A-A', overlying  
421 the Egmond Ground Formation (Fig. 6). One channel is observed descending from the basal reflector  
422 of Unit I, suggesting channel incision either pre-dates or is broadly contemporaneous with the  
423 formation of the unit. The majority of the unit is tabular with thicknesses averaging between 3-5 m  
424 (c.4-7 ms two-way travel time; 1700 m/s assumed). The unit includes some irregular and  
425 discontinuous reflectors suggestive of lithologic and/or structural heterogeneity (Fig. 6 – south).  
426 One of these reflectors separates the fill in the channel from that of the overlying unit. In the far  
427 south the unit thickens and exhibits a ridge/wedge-like structure, rising up to where it is truncated at  
428 sea bed. Profile B-B' shows the southern extension of this thickened feature. The data along profile  
429 B-B' also suggest that this feature is a buried wedge (comprising SUs I & II) which has been slightly  
430 truncated/eroded at seabed, presumably by Holocene/modern marine erosion. This buried wedge  
431 corresponds to the subtle bathymetric high which is associated with NR2 observed on regional  
432 bathymetry data (Fig. 9).

433 Overlying SU I, **SU II** is a broadly tabular lens of sediment (c.4-8 m thick). Locally, a deep channel is  
434 incised from the basal reflector of SU II, and this channel appears to have been further exploited by  
435 later Holocene fluvial action (Fig. 6) (e.g. Fitch et al., 2005). SU II exhibits a highly  
436 chaotic/transparent, low-acoustic energy character which is interpreted to reflect a predominantly  
437 homogeneous deposit such as a diamicton (Stewart and Stoker et al., 1990; Ó Cofaigh et al., 2005).  
438 South of the large sand bank (yellow), SU II outcrops at/near seabed, underlying mobile seabed  
439 sediments. Profile B-B' suggests that Unit II mantles, and builds upon SU I's wedge-like structure in

440 the south, and is also truncated at seabed. SU II also extends farther south than SU I, which appears  
441 to pinch out just south of the wedge (Fig. 7). SU II extends to the north beneath the sediment bank  
442 where its stratigraphic association with the overriding/abutting SUs III & IV is difficult to assess due  
443 to the acoustic masking effect, and seabed multiple of the sediment bank (Fig. 6).

444 **SU III** does not appear to directly overlie SU II (Fig. 6) and appears to persist only in the northern half  
445 of profile A-A', overlying the Egmond Ground Formation. SU III is thin and roughly tabular (2-3 m  
446 thick) but thickens southward to form a buried wedge structure (up to c.12 m thick) which is  
447 exposed and truncated at/near seabed. As with SU II, SU III exhibits a highly-chaotic/transparent  
448 acoustic character. The wedge-shaped seismostratigraphic unit is interpreted as a constructional  
449 landform rather than an erosive feature because the irregular top surface is more suggestive of a  
450 constructional origin than incision. This feature also exhibits a similar morphology to the buried  
451 ridge within SU I at the southern end of profile A-A' and B-B'. This apparent buried ridge  
452 corresponds to, and sub-crops just north (c.2 km) of NR4 on the northern-most BSW (Fig. 9).  
453 Towards its southern limit, the stratigraphic boundary between SU III and the overriding SU IV is not  
454 entirely clear, with a channel incised into both units. SU III however appears to pinch-out against its  
455 flat basal reflector, atop the Egmond Ground Formation.

456 **SU IV** is somewhat distinct from the other units in its variability of geometry and acoustic character.  
457 Unit IV broadly mimics the form of the underlying Unit III, but is interpreted to extend both farther  
458 to the north and south. Towards the north, SU IV drapes SU III, and while thin, the irregular top-  
459 surface forms a series of ridge or mound-like structures. Where SU III thickens, SU IV shows  
460 onlapping reflector terminations. Several channels are part of the basal reflector of SU IV which are  
461 cut into SU III (and deeper units) in the north, potentially infilled with the type of sediment which  
462 constitutes the overlying Unit V. In the south, the stratigraphic relationships with SUs II and III are  
463 more ambiguous because attenuation of the acoustic signal by an overlying sand bank. SU IV  
464 comprises more laterally-continuous reflectors than other units, exhibiting a higher-amplitude  
465 acoustic character. There are several channels eroded into and from its base. Just south of  
466 bathymetrically-interpreted NR3 and underlapping SU V (NR4) (Fig. 6), a large infilled channel (c.12  
467 m deep) exhibits bedded, conformable reflectors (marked by G.C. on Fig. 9). We interpret the  
468 acoustic character of this channel infill to reflect water-lain deposits. The location of this infilled  
469 channel corresponds with a narrow bathymetric depression, which just south of NR3 extends  
470 discontinuously to the east of profile A-A'. Other seismic data that cross this depression (and  
471 similarly, south of NR4) reveal further infilled channels, suggestive of connected channel networks  
472 between the upstanding bathymetric wedges (Fig. 9)

473 **SU V** is the highest seismostratigraphic unit within the assemblage and occasionally crops-out within  
474 the seabed where not covered by a veneer of active seabed sediments (Tappin et al., 2011). Along  
475 profile A-A' SU V is broadly tabular in form, ranging in thickness from 6-10 m, and exhibits a  
476 complex/transparent acoustic character suggestive of massive, structureless diamicton. In the  
477 north, several erosional channels are cut from its base and into the underlying stratigraphy. In the  
478 north, a partly-infilled channel is exposed at seabed, and is the northern tip of one of the large  
479 seabed incised deeps, which is oriented oblique to this seismic profile (Fig 2). The southern margin  
480 of SU V is characterised by a pronounced southerly-dipping bathymetric slope. The top of this slope  
481 marks the position of NR4 and the southern edge of a BSW (Fig. 9).

482 Collectively, SUs III-V together form a wedge-like structure in profile, thinning and shallowly-dipping  
483 northwards, with a relatively steep and abrupt slope in the south. On this basis, and as observed  
484 elsewhere (e.g. SUs I & II corresponding to NR2 (Figs. 7, 9) we infer that the broad, arcuate sediment  
485 wedges observed on the bathymetry data are entirely formed by the sequential stacking of  
486 seismostratigraphic units (e.g. units III-V), which cores confirm comprise BBF till. A further  
487 observation is that along profile A-A', the wedge-like package of SU V thins over buried ridge of SU III  
488 and IV, extending c.2 km farther to the south where it is marked by NR4. Bathymetry data reveal  
489 that NR4 locally intersects NR3 near profile A-A', providing an indication that the depositional  
490 regime responsible for formation of SU V (NR4), encroached on the pre-existing wedge associated  
491 with SU III (NR3).

### 492 **3.3.2 Profile C-C'**

493 Profile C-C' is included here to demonstrate that the architectural trends (stacked till wedges)  
494 apparent along profiles A-A' and B-B' are not geographically confined, but are representative of the  
495 whole study area (Fig. 8). The data along profile C-C' (2008/5 line 9rev) are of poorer quality  
496 (acquired in winter), but still reveal the southern margin of the till wedge associated with NR3. In  
497 the subsurface it is clear that the broader wedge is a composite feature comprising at least two SUs,  
498 both of which comprise till (Fig. 9). The lower most SU exhibits a broad ridge-like cross-sectional  
499 profile, and incorporates some internal structure as well as several reflectors. Ramping up onto the  
500 lower SU, the overlying SU exhibits a similar acoustic character (massive/transparent) and extends  
501 farther north to where it is cut by a seabed incised deep ('Sole Pit'). Farther north (c. 2 km) along the  
502 seismic line from which profile C-C' is extracted, the lower SU thins and pinches out against the  
503 planar basal reflector.

## 504 **3.4 Interpretation of geomorphic and shallow geological record**

505 On the basis of the bathymetric evidence we identify close morphological affinities between several  
506 distinctive positive-relief landforms, together with the incised deeps across the region. This new

507 geomorphological record has drawn attention to previously unrecognised seismostratigraphic  
508 relationships in the subsurface. Below we combine observations of the bathymetry, seismic, and  
509 sediment core data to produce an integrated interpretation of glacial features preserved at seabed  
510 and in the shallow subsurface.

### 511 **3.4.1 Till wedges and moraines – Record of glacier sub-marginal processes**

512 Listed in decreasing size, the positive-relief features (of non-marine origin) observed in the  
513 bathymetry data are: i) the regional-scale bathymetric high extending E-W across the study area; ii)  
514 several BSWs that together make-up the regional high; and iii) the NRs that delimit the southern  
515 margins of the arcuate BSWs (Figs. 2, 9, 10). Sediment cores (Fig. 9) reveal that these arcuate BSWs  
516 comprise Bolders Bank Formation (BBF) which has been interpreted as subglacial till, and that the  
517 NRs 1-4 also comprise glacial deposits, altogether demonstrating a glacial origin for this landform  
518 assemblage. Re-analysis of BGS shallow seismic data reveal that the sub-surface unit previously  
519 mapped singularly as the BBF (e.g. BGS, 1991; Cameron et al., 1992) can be divided into at least five  
520 separate seismostratigraphic units (SUs), that have been progressively and shallowly stacked from  
521 south to north over large lateral distances (10's kilometres), indicating younging to the north (Fig.  
522 10b).

523 Critically, the architecture (e.g. stacked strata and buried wedges) and extent of these  
524 seismostratigraphic units correspond to the position and character of the landform assemblages  
525 observed on the seabed (Figs. 6, 9, 10b). For example, NR 1 corresponds very well with the  
526 previously mapped seismostratigraphic extent of the BBF and the southern distribution of cores  
527 comprising BBF. The shallow south-to-north stack of SUs over large lateral distances (> 10-20 km)  
528 forms composite sub-surface (cross-sectional) wedges that also fully account for the extent and  
529 morphology of the broad arcuate wedges observed at seabed. Along profiles A-A' (Fig. 6) and B-B'  
530 (Fig. 7) the stacked succession of SUs I and II corresponds to the broad sediment wedge (IM 2 – Fig.  
531 10b) which has NR2 along its southern margin (Fig. 9). Similarly, SUs III-V account for the wedge (IM  
532 4 – Fig. 10b) associated with NR4 (Figs. 6, 9), and the stacked SUs on profile C-C' comprise the wedge  
533 (IM 3- Fig. 10b) associated with NR3 (Figs. 8, 9).

534

535 Based on the morphological, sediment core and seismic evidence, together with reference to  
536 findings from other glaciated basins, including the northern North Sea (e.g. Bradwell et al., 2008), we  
537 interpret that the broad sediment wedges (BSWs) and narrow ridges (NRs) (1-4) relate to subglacial  
538 and ice marginal processes acting along several terminal positions of the former North Sea Lobe of  
539 the BIIS (cf. Boulton 1996a, b; Evans & Thomson 2010; Boston et al. 2010; Evans et al., 2012; Eyles  
540 et al., 2011). We interpret the NRs (1-4) delimiting the southern edge of the BSWs as terminal  
541 moraines, which mark successive ice-marginal still-stands (e.g. Colgan et al., 1999, 2003; Shaw et al.,

542 2007; Dowdeswell et al., 2008). Several isolated loop-shaped moraines mapped south of moraine-  
543 ridge 3 are interpreted as evidence of either a localized marginal re-advance, or a general saw-tooth  
544 pattern that is common to lobate ice sheet margins within enclosed basins and piedmont settings  
545 (i.e. radial crevassing) (Fig. 9) (e.g. Price 1970; Evans & Twigg 2002; Kalm, 2012; Lee et al., 2013;  
546 Evans et al., 2015; Eyles et al., 2015).

547 The BSWs, and by extension the shallow stacked SUs (e.g. SUs I, II, III, V), are interpreted as sub-  
548 marginal till wedges formed by complex accretionary processes that resulted in the accumulation  
549 and thickening of glacial sediment inboard of the separate ice margins (Figs. 6,9) (Boulton et al.,  
550 1996b; Evans and Hiemstra, 2005; Eyles et al., 2011; Evans et al., 2012; Lee et al., 2016). We suggest  
551 that each of the BBF SUs, with the exception of SU IV, which incorporates a high proportion of  
552 channels, relate to individual still-stand episodes where incremental till thickening occurred towards  
553 the ice margin (thinning up-glacier), producing the BSWs now apparent at seabed (Ice-margins 1-4:  
554 Figs. 6, 9, 10) (Leysinger-Vieli & Gudmundsson 2010; Eyles et al. 2011; Evans et al., 2012).

### 555 **3.4.2 Tunnel valleys**

556 Consistent with previous investigations in the region, we interpret the large seabed incised deeps (U-  
557 shaped in cross-section; scoop-shaped in longitudinal profile) as glacial tunnel valleys (e.g. Donovan,  
558 1972; Tappin et al., 2011; Van der Vegt et al., 2011), and that these features were likely formed due  
559 to erosion by over-pressurized subglacial meltwater (e.g. Kehew et al., 2012). What has not been  
560 previously recognized is that the northern and southern limits of individual tunnel valleys are  
561 coincident with the equivalent northern and southern edges of the BSWs (i.e. discrete ice sheet  
562 margins) into which they are incised (Figs. 9, 10). Because of this association, tunnel valleys are  
563 geographically grouped, and are found incising three of the four arcuate wedges. Tunnel valleys  
564 associated with the northern two ice margins 3 and 4 demonstrate this relationship most clearly,  
565 with only one smaller, apparently connected channel system relating to ice margins 1 and 2.

566 We interpret that this landform association demonstrates a clear genetic relationship between the  
567 emplacement of the till wedges at ice margins 2-4, and the meltwater erosion that led to the  
568 formation of the tunnel valleys. As such the landform assemblage forms a sub-marginal glacial  
569 landsystem similar to those of modern active temperate glacier lobes and not unlike of ancient  
570 terrestrial ice sheet margins.

### 571 **3.4.3 Coast-parallel offshore ridges**

572 The presence of small moraine ridges in Holderness (Evans & Thomson, 2010) originally drew our  
573 attention to a potentially related series of thin ridges observed offshore of the Holderness coast  
574 (Figs. 5, 9, 10a). The similar orientation and dimensions of these offshore ridges hints at a near  
575 seamless continuation of the terrestrial moraine belt, providing a high-resolution record of ice sheet  
576 retreat in the region. Several factors however suggest that these features are unlikely to be primarily

577 of glacial origin: 1) The offshore ridges exhibit a very 'fresh' geomorphic character with slopes up to  
578 25°. Such excellent preservation seems unlikely in this shallow, wave-influenced high-energy  
579 hydrodynamic environment, where mean tidal current velocities reach nearly 2 m/s (Tappin et al.,  
580 2011); 2) Several offshore ridge specimens are observed immediately adjacent to the modern coast  
581 (within c.200 m) (Google Earth satellite imagery also suggests they are also found in the intertidal  
582 zone where not directly mapped acoustically). Intense coastal erosion and sediment bar migration is  
583 known to occur along this coastline (e.g. Pringle, 1985) suggesting that ridge formation is more likely  
584 linked to modern, or perhaps relict Holocene coastal processes.

585 Despite their probable marine origin, these ridges still may reflect a glacial influence, albeit  
586 indirectly. Fig. (5) shows that the crisp narrow ridges sit atop a broader, more diffuse fabric of c.NW-  
587 SE oriented ridges with intervening lows. This underlying fabric appears to control the location and  
588 orientation of the narrow ridges (i.e. sitting atop the rugged, broader ridges), and this pre-existing  
589 topography itself may reflect former glacial processes. In other words the more modern marine  
590 bedforms have preferentially formed over relative bathymetric highs, and therefore mimic the  
591 orientation of the underlying topography (e.g. potential moraine belt). This offshore record may help  
592 understand the topographic evolution of Holderness, but focussed and direct sampling of these  
593 features is required to better inform interpretations of their origin.

## 594 **4 Discussion**

595 Despite the amount of published literature from adjacent onshore sequences in East Yorkshire and  
596 Norfolk (e.g. Catt, 2007; Moorlock et al., 2008; Evans & Thomson, 2010; Bateman et al., 2015; Evans  
597 et al., 2016), comparatively little is known about the equivalent offshore record of the last glacial  
598 cycle. The accumulated evidence derived from *in situ* marine data in the southern North Sea has  
599 largely precluded MIS 2 glaciation from being characterised with any greater specificity than as a  
600 single event. The extensive BGS programme of geophysical surveying and coring during the 1970's  
601 through early 1990's provided a coarse (though broadly accurate) characterisation of the Quaternary  
602 sediments in the region (e.g. Cameron et al., 1992), but inadequate dating of core material  
603 combined with an insufficiently detailed seismostratigraphic model on which to hang existing dates  
604 has inhibited progress. There has been some effort to consider the existing offshore record in  
605 reference to the more nuanced onshore evidence (e.g. Boston et al., 2010), but there has been  
606 surprisingly little work conducted to re-analyse the offshore data (e.g. provenance -Davies et al.,  
607 2011). One important exception to this is the work by Carr et al. (2006) (described in greater detail  
608 within Introduction), who through provenance and micromorphological analysis found evidence of  
609 at least two stages of glaciation impacting this part of the southern North Sea (Fig. 1). Our results are  
610 broadly compatible with this work (i.e. more than one incursion of ice into the region), but through

611 the identification of new geomorphological and stratigraphic relationships, we are able to describe  
612 and map a more detailed and spatially accurate record of glaciation within the southern North Sea.

#### 613 4.1 Offshore landform associations, ice sheet dynamics, and relative event 614 chronology

615 The series of broad arcuate till wedges (BSWs) and associated moraines (NRs) observed on the  
616 bathymetry data represent several terminal positions of the former North Sea Lobe of the British  
617 and Irish Ice Sheet (BIIS) (Figs. 9, 10a). Supporting this, and providing relative chronological control,  
618 shallow stacked seismostratigraphic units (SUs) within the BBF are observed to directly correspond  
619 to the position and extent of specific arcuate wedge/moraine complexes (ice-margins 1-4) (Figs. 6-8,  
620 10b). These discrete ice margins also show clear affinities with the region's tunnel valleys in that  
621 their location and orientation is correlated with (and bracketed by) the position of the BSWs,  
622 suggesting a formational interdependence between the landforms as a sub-marginal glacial  
623 landsystem (e.g. Colgan et al., 2003; Jørgensen and Sanderson, 2006). The arcuate till  
624 wedge/moraine complexes indicate that the former ice margins were lobate in plan-view, with the  
625 tunnel valleys radiating out from the centre trunk of the ice stream and intersecting the  
626 reconstructed margins approximately perpendicularly (Fig. 10). This inferred association, together  
627 with the maturity of the observed landforms (i.e. the extent and thickness (up to c.15 m) of  
628 individual till wedges; size of tunnel valleys up to c.80 m deep below surrounding seabed), indicates  
629 that these landform assemblages (till wedges and corresponding groups of tunnel valleys) were  
630 formed during separate still-stand episodes of the North Sea Lobe as the ice margin was stationary  
631 for several periods of time before retreating and stepping back to the north. As such they represent  
632 inset sequences of sub-marginal glacial landsystems similar to those recognized in a variety of  
633 ancient terrestrially-based ice sheet marginal settings (e.g. Colgan et al. 2003; Evans et al., 2006,  
634 2014; Jennings, 2006; Ó Cofaigh et al. 2010; Eyles et al. 2011).

635 Glacier sub-marginal thickening of subglacially deforming sediment, acting in tandem with other  
636 subglacial advection processes (cf. Alley et al. 1997), to produce incrementally stacked till wedges  
637 has been demonstrated by empirical-based theory (Boulton, 1996a, b), modern process observations  
638 (Evans & Hiemstra 2005) and numerical modelling (Leysinger-Vieli & Gudmundsson 2010). Such  
639 studies reveal a clear linkage between moraine construction and subglacial till emplacement  
640 processes, wherein the stratigraphic architecture of repeated ice-marginal oscillations during slow  
641 recession or dynamic oscillations of quasi-stable glacier lobes is manifest as superimposed, lobate-  
642 shaped till wedges. This model of till emplacement has been applied to the landform-sediment  
643 associations of the southern margins of the Laurentide Ice Sheet by Boulton (1996a, b), Patterson  
644 (1997, 1998), Jennings (2006), Evans et al. (2008, 2012, 2014) and Ó Cofaigh et al. (2010) as well as

645 the onshore till sequences in eastern England by Boston et al. (2010), Evans & Thomson (2010) and  
646 Lee et al. (2016). Importantly, these zones of incremental thickening and marginal till wedges involve  
647 net vertical accretion of subglacial deposits, which is critical to the preservation of meltwater  
648 sediments in canal fills, which are observed to thicken towards eskers and/or ice-contact  
649 subaqueous fans or grounding line fans on Holderness (Evans et al., 1995; Evans & Thomson 2010)  
650 and the Durham coast (Davies et al. 2009). Evidence for the preservation of similar discontinuous  
651 meltwater features appears to be manifest in the few internal laterally-continuous reflectors in what  
652 otherwise are homogenous diamictons. Additionally, as the seabed tunnel valleys are observed to  
653 incise into and below respective till wedges, e.g. the uppermost unit of the BBF (seismic unit V) (Fig.  
654 6), we infer that valley incision and till deposition occurred pene-contemporaneously.

655 Seismostratigraphic evidence demonstrates that the till wedge/moraine complexes in the south are  
656 predominantly associated with stratigraphically deeper and presumed older glacial deposits. We  
657 interpret therefore that the four observed till wedge/moraine complexes visible in the bathymetry  
658 data (Figs. 6, 9, 10) record the phased occupation and retreat of the North Sea Lobe from south to  
659 north, with the oscillating ice margin holding at least four major still-stand positions before  
660 retreating north out of the study area. In the south, SU II overlies and appears to extend farther  
661 south than SU I (Figs. 6, 7). This suggests that the oldest stratigraphic member (SU I) is in fact  
662 associated with Ice-margin 2, and that SU II potentially records a significant re-advance that brought  
663 the oscillating margin of the NSL to its most southerly extent (e.g. encroaching on North Norfolk;  
664 Roberts et al. in prep). Higher quality, and more densely distributed seismic data will be required to  
665 confirm this potential re-advance signature in the south. Isolated loop-shaped moraines extending  
666 south beyond Ice-margin 3 indicate transient and minor re-advance, but the seismic data presented  
667 in Figs. (6, 7) provide evidence of what appears to be another significant re-advance associated with  
668 the youngest glacial episode and related to Ice-margin 4. Along profile A-A', the buried sediment  
669 wedge of SU III is truncated and overlain by sediments of SU V, which corresponds with Ice-margin 4  
670 and the northern-most assemblage of tunnel valleys (Fig. 9). Elsewhere in the offshore environment,  
671 Ice-margin 3 is located farther south than Ice-margin 4, but at the crossing of profile A-A' the two  
672 landform assemblages are convergent. In accordance with this geomorphic configuration and the  
673 stratigraphic observations, we interpret that SU III is associated with Ice-margin 3. With SU V over-  
674 riding and extending farther south than SU III along profile A-A', this provides evidence of ice-sheet  
675 re-advance, which at least locally overrode the deposits of the previous ice sheet margin.

676 The combined stratigraphic and geographic position of tunnel valleys provides further constraint on  
677 the relative age of these landform assemblages. Like the seabed incised deeps, we interpret deeply  
678 incised channels buried in the subsurface as tunnel valleys because they are cut from stratigraphic

679 units comprising BBF subglacial till (Fig. 6). One exception is observed along profile A-A' where the  
680 channels incised from SU IV appear (laminated, conformable) more to be likely associated with ice-  
681 marginal/proglacial erosion from the still-stand positions marked by Ice-margins 3 or 4. For those  
682 interpreted as tunnel valleys, we find that the valleys eroded from the deeper SUs (I & II) are  
683 observed in the south, whereas channels in the north are eroded from the higher (and younger) SUs  
684 (III-V), including the northern reach of the seabed-exposed tunnel valley eroded into seismic-unit V  
685 (Figs. 6, 9, 10). This argument that the stratigraphic position of the tunnel valleys is indicative of  
686 relative age and retreat direction is dependent on the assumption that subglacial meltwater  
687 conduits would have been concentrated near the ice margin (cf. Hooke and Fastook, 2007; Storrar et  
688 al., 2014), and the close association between the tunnel valley groups with Ice-margins 2-4, together  
689 with observations from other terrestrial lobate ice margins (e.g. Colgan, 1999; Colgan et al., 2003),  
690 appear to support this hypothesis.

691 The largest tunnel valleys are found within the northern-most assemblage (e.g. Inner Silver Pit and  
692 Sole Pit), which notably coincides with the largest and most morphologically pronounced (and  
693 stratigraphically youngest) Ice-margin 4 (Figs. 6, 9, 10). This may indicate longer residence time at  
694 this margin allowing for increased thickening and erosion (e.g. Boulton et al., 2001), better  
695 preservation potential, or alternatively that sediment accumulation and meltwater production at  
696 this northern-most position were for some reason greater at this time. With respect to individual  
697 margins we also observe that the spacing between tunnel valleys appears to be proportionate to  
698 their size, and by inference, meltwater discharge. To investigate whether this apparent dependency  
699 is valid, we measured the cross-sectional area (measured 5 km up-glacier from moraine) as well as  
700 the distance between tunnel valleys along the northern-most moraine 4 (Fig. 11). We utilised the  
701 smallest distance measured between each tunnel valley to assess the relative influence of each  
702 meltwater conduit (i.e. catchment). There are seven mapped tunnel valleys along this till  
703 wedge/moraine complex, but we only analysed the inner five as the Sand Hole and Well Hole tunnel  
704 valleys are unconstrained in the far west and east respectively (Fig. 2). A simple regression analysis  
705 demonstrates a positive linear relationship ( $R^2 = 0.986$ ) between tunnel valley spacing and cross-  
706 sectional area (i.e. discharge). While acknowledging that the small sample population requires that  
707 these results are treated with some uncertainty, this analysis does suggest a correlation and  
708 proportional relationship between the two variables, which is consistent with theoretical predictions  
709 of meltwater drainage and the spacing of associated landforms (e.g. Boulton et al., 2007; Hewitt,  
710 2011; Dowdeswell et al., 2015).

711 The southern rims/outlets of the tunnel valleys commonly extend 2-5 km beyond the till  
712 wedge/moraine complexes, suggesting that subglacial meltwaters were strongly focussed towards

713 (and confined by) individual tunnel valleys until reaching the ice margin, where they were released  
714 (Figs. 9, 10). It is anticipated that this mid-latitude palaeoglaciological system would have produced  
715 significant volumes of meltwater (e.g. Toucanne et al., 2010), and indeed the large size of the tunnel  
716 valleys suggests that it did. However, because of the study area's submarine setting, the  
717 preservation potential for other glacifluvial landforms (e.g. fans) and glacifluvial deposits is low, and  
718 few are found regionally (Cameron et al., 1992). Due to the shallow nature of the seabed and  
719 proximity to the coast, the study area is characterised by very high-energy hydrodynamic conditions  
720 (e.g. ubiquitous mobile sediment waves) and has since been drowned during the Holocene marine  
721 transgression (Uehara et al., 2006; Sturt et al. 2013; Ward et al., 2016). However, one consequence  
722 of this study is that the shallow depressions between the till wedges may have hosted glacifluvial  
723 pathways, and the channels observed in seismic unit IV seem to indicate that such deposits may be  
724 preserved here (Fig. A-A'). Despite the relative absence of depositional landforms and glacifluvial  
725 deposits, the apparent correlation between tunnel valley size and spacing indicates that they served  
726 as the primary control on regulating meltwater drainage (Fig. 11), and suggests that the till  
727 wedge/moraine complexes served as an effective dam to meltwater escape, with meltwaters being  
728 routed towards tunnel valleys within catchments that were proportional to the size of each valley  
729 (e.g. Boulton et al., 2007).

730 Due to the unambiguous link between the tunnel valleys and the till wedge/moraine complexes  
731 associated with the BBF, we infer that the location, pattern, and morphology of the tunnel valleys  
732 may be satisfactorily attributed to Late Devensian (MIS 2) glaciation alone. However, whether the  
733 valleys are multi-generational features and pre-disposed by previous valley incision from older  
734 glacial periods (e.g. MIS 12) is not immediately clear.

735 In order to significantly improve the geomorphological and stratigraphic record of the region, higher-  
736 resolution swath bathymetry and better quality 2D and/or 3D seismic data over extensive areas will  
737 be required. Further to this, targeted absolute dating will be necessary to tie this combined  
738 reconstruction of sub-marginal ice sheet dynamics and evolving spatial configurations of the NSL, to  
739 the broader activity of the BIIS. There is existing evidence however, that the incursion of the NSL into  
740 the region was a relatively late phenomenon, bracketed between about 21 ka and 15 ka (Batemen et  
741 al., 2015). Central to accounting for this diachronous event will be to understand the interaction  
742 between the BIIS and the Fennoscandian Ice Sheet (FIS) in the southern North Sea, as is becoming  
743 clearer in the northern North Sea (e.g. Bradwell et al., 2008; Sejrup et al., 2016). An important next  
744 step towards this aim will be to characterise the relationship of the NSL with the Dogger Bank (e.g.  
745 Cotterill et al., in review). The study presented here demonstrates the dynamic nature of the NSL  
746 when it was at or near its maximum southern extent; but what did it encounter in the Dogger Bank

747 area; how far did it extend when it first impinged on the region; and how did it interact with the  
748 Dogger Bank as it actively retreated back to the North and West?

#### 749 **4.2 Stratigraphic correlation with the onshore record**

750 The age and dynamics of the Late Devensian glaciation in Eastern England are relatively poorly-  
751 constrained but the chronology of regional glaciation is the focus of significant recent and ongoing  
752 research (Bateman et al. 2011, 2015; Evans et al., 2016; Roberts et al. in prep.). This study however  
753 provides a crucial link between the offshore record and onshore successions in East Yorkshire (Catt &  
754 Penny, 1966; Catt, 2007; Boston et al., 2010; Evans & Thomson, 2010; Roberts et al., 2013; Bateman  
755 et al., 2015) and north Norfolk (England and Lee, 1991; Pawley et al., 2006; Moorlock et al., 2008),  
756 enabling the first regional-scale interpretation of the North Sea lobe of the Last British-Irish Ice Sheet  
757 within the Southern North Sea (Clark et al., 2012).

758 The southern-most extent of this ice advance is indicated by Ice-margin 1 (SU1) and is tentatively  
759 correlated with the onshore occurrence of the Holkham Till in north Norfolk (Pawley et al., 2006;  
760 Roberts et al. in prep.) and the oldest (“advance till”) units of the Skipsea Till in East Yorkshire (Figs.  
761 9, 10) (Catt 2007; Evans & Thomson 2010). Onshore deposits in north Norfolk include thin beds of  
762 diamicton and outwash sand and gravel locally forming morainic landforms and kame mounds, on  
763 the northern flanks of low Chalk hills (England and Lee, 1991; Pawley, 2006; Pawley et al., 2006;  
764 Moorlock et al., 2008; Roberts et al. in prep). Ice damming of northward-draining chalk rivers,  
765 including the Stiffkey and Heacham rivers, led to the development of several impounded lake basins  
766 and localised drainage diversions (Brand et al., 2002; Moorlock et al., 2008). The position of the ice  
767 margin in the modern area of the Wash and Fen basins between northwest Norfolk and Lincolnshire  
768 remains unclear, with evidence presumably, having been either buried beneath Holocene deposits  
769 or removed by fluvial and/or marine processes. Alternatively, the clay-rich substrate (Kimmeridge  
770 Clay – Jurassic bedrock) within the Wash (as opposed to the chalk substrate in adjacent areas) may  
771 have promoted ice-bed decoupling and southward ice flow. Therefore, the ice margin may have  
772 been situated to the south of the modern coastline within the Wash.

773 Combined seismostratigraphic and geomorphic evidence presented in this study suggests however  
774 that this most laterally-extensive episode of glaciation, does not coincide with the first ice advance  
775 into the region (i.e. SU1 overlaps SUI and extends farther south to Ice-margin 1). The  
776 stratigraphically deeper and presumed older SU1 is instead associated with Ice-margin 2 (Figs. 6, 9),  
777 indicating that deposits associated with this first encroachment of Devensian glaciation into the  
778 region did not reach the north Norfolk coast. Projecting Ice-margin 2 towards the East Yorkshire  
779 coast demonstrates good alignment with a previously mapped moraine belt in East Yorkshire (Figs.  
780 9, 10), and is also potentially associated with the various advance and retreat till wedges of the

781 Skipsea Till which crops-out extensively across the region (Boulton 1996a, b; Evans and Thompson,  
782 2010; Boston et al., 2010). An alternative hypothesis is that this oldest Late Devensian glacial  
783 episode (SUI; Ice-margin 2) is associated with the Basement Till (e.g. Catt et al., 2007), which  
784 underlies the Skipsea Till in the north of Holderness (Evans and Thompson, 2010). This hypothesis is  
785 also considered viable due to: i) the correlation between the seismostratigraphic framework  
786 presented here with the glacial depositional model presented by Evans & Thompson (2010), and ii)  
787 the interpreted extent of the Basement Till (based on borehole analysis) broadly corresponds with  
788 the landward projection of Ice-margin 2 (Figs. 9, 10). Previously, Eyles et al. (1994) presented amino  
789 acid dates that supported a Late Devensian origin for the Basement Till, and Evans and Thompson  
790 (2010) indicated that this could be accommodated within their depositional model for East  
791 Yorkshire. The stratigraphic position of the Basement Till, via its relationship to the Sewerby (MIS 5e)  
792 raised beach, remains to be elucidated (Catt, 2007).

793 Ice margins 3 and 4 record a stepped northwards retreat of the ice margin. In East Yorkshire, Ice-  
794 margin 3 likely further corresponds to the “retreat till” units of the Skipsea Till (Evans & Thomson  
795 2010). Ice Margin 4 records the final known offshore position of the ice margin and correlates  
796 onshore with the deposition of the Withernsea Till and formation of the onshore morainic ridges  
797 (Figs. 9, 10) (Evans & Thomson, 2010). The maximum onshore ice limit is situated on the reverse  
798 dip-slope of the north-south striking Chalk bedrock which forms the Lincolnshire and Yorkshire  
799 Wolds (Catt, 2007; Evans and Thomson, 2010). To the north of the Humber Estuary in Holderness,  
800 the glacial succession thickens, comprising a complex sequence of diamictos, ice-contact lacustrine  
801 and proglacial outwash sediments (Catt and Penny, 1966; Madgett and Catt, 1978; Evans et al.,  
802 1995; Catt, 2007; Evans and Thomson, 2010; Boston et al., 2010; Roberts et al., 2013). Detailed  
803 lithological analyses demonstrate that the diamictos were deposited by ice flowing down the east  
804 coast of England from southern and eastern Scotland (Busfield et al., 2015) with variations in bulk  
805 composition reflecting spatial changes in the predominant source of substrate entrainment along  
806 the ice flow-tract (Boston et al., 2010). Eastwards retreat of the ice margin led to the formation of a  
807 succession of morainic ridges (Evans and Thomson, 2010) which may continue offshore into the  
808 Coast-parallel offshore ridges (Figs. 9, 10). In fact, combining the previously mapped terrestrial  
809 record (e.g. moraines) with the newly-mapped seabed geomorphology, suggests that the entire  
810 landscape of Holderness itself may be a large moraine complex. Ice-margin 3 can be extrapolated to  
811 project up the Humber Estuary, and Ice-margin 4 onto Holderness, providing a credible origin for its  
812 position, topography, and orientation (e.g. causes River Humber to deflect southeast). Recently  
813 published OSL dates from coastal sections in Holderness indicate that the area was initially glaciated  
814 between 21 and 19 ka but was ice-free by about 15 ka (Bateman et al., 2015). Further absolute

815 chronological data is anticipated from the recent BRITICE-CHRONO sampling campaign, providing  
816 useful dated reference points with which to constrain the spatiotemporal reconstruction presented  
817 here (e.g. Roberts et al., in prep).

## 818 **Conclusions**

819 The southern North Sea serves as an interesting 'marine' setting to study glaciation, as not only did  
820 the region lie above sea-level during the last MIS 2 glaciation, but ice was directed away from the  
821 ice-sheet centre within an epicontinental basin, rather than directly towards the marine margin. In  
822 this regard, the southern North Sea palaeoglaciological system is more analogous to terrestrial ice  
823 lobes than marine-based ice masses.

824 Within this study, new bathymetry data have been used to identify and describe an extensive series  
825 of glacial landforms relating to the phased occupation and retreat of the North Sea Lobe (NSL), the  
826 southern-most component of the last British-Irish Ice Sheet east of Britain. Mapping these  
827 landforms has in-turn drawn attention to related, and previously unrecognized, broadscale  
828 architectural patterns within existing shallow seismic data. Characterising this combined landform  
829 and seismostratigraphic assemblage has led to the following observations:

- 830 • Apart from superficial Holocene sediment banks and waves, glacial landforms are  
831 responsible for the conspicuous variation in the region's seabed morphology. Extending ~E-  
832 W across the study area, a series of broad arcuate wedges are delimited at their southern  
833 margins by relatively narrower moraines. Together, these landforms represent several  
834 terminal positions (lobate in plan-view) of the former NSL (Ice-margins 1-4);
- 835 • Sediment cores and shallow seismic data reveal that each of the broad arcuate wedges  
836 comprise subglacial till of the Bolders Bank Formation (BBF), which has here (for the first  
837 time) been subdivided into at least five separate seismo-stratigraphic units. Importantly, the  
838 architecture of these units (i.e. shallow stacked wedges) is consistent across the study area,  
839 and corresponds to the position and character of the arcuate wedge/moraine complexes  
840 observed at seabed;
- 841 • These broad sediment wedges (observed at seabed and in the sub-surface) are interpreted  
842 as sub-marginal till wedges, formed by complex accretionary processes inboard of several  
843 still-stand ice margins (e.g. Ice-margins 1-4). This glacial landsystem is similar to examples  
844 previously recognized in terrestrially-based ice sheet marginal settings (e.g. southern  
845 Laurentide);
- 846 • Discrete groups of subglacial tunnel valleys are incised ~perpendicularly into the lobate till  
847 wedge/moraine complexes, with the northern and southern rims of the tunnel valleys  
848 coincident with the northern and southern margin of the respective till wedge/moraine

849 complexes. This close and repeated correlation indicates a clear genetic relationship  
850 between the position of individual ice margins and the origin of the tunnel valleys. Further  
851 to this, we observe a significant relationship between the size (i.e. inferred discharge) of the  
852 tunnel valleys and the spacing between them, suggesting that meltwater was organised  
853 within catchments that were proportional to the size of each tunnel valley, conforming with  
854 theoretical predictions of meltwater routing in mid-latitude glaciological systems;

- 855 • Seismic data provide constraint on the relative event chronology of the NSL, with the  
856 subdivided BBF seismostratigraphic units progressively and shallowly stacked from south to  
857 north (generally younging to the north). There are also however, several clear examples of  
858 ice sheet re-advance; for example, the oldest stratigraphic unit (Seismic-unit I) corresponds  
859 to the position of Ice-margin 2, which was over-ridden to the south by an ice lobe recorded  
860 by Seismic-unit II (southern-most ice-margin 1). Overall this is indicative of an oscillating ice  
861 sheet margin that occupied several lobate still-stand positions prior to its retreat from the  
862 region;
- 863 • We demonstrate that the more detailed, and spatially accurate reconstruction presented  
864 here (based on in situ data from within the southern North Sea) is compatible with existing,  
865 more disparate terrestrial records of MIS 2 glaciation. Ice margins mapped offshore are  
866 geographically well correlated to the fragmentary onshore limits, and further to this,  
867 offshore seismostratigraphic associations place these terrestrial limits into a clearer  
868 regional-scale event chronology.
- 869 • This new reconstruction of the NSL provides an important new framework for understanding  
870 the late-stage behaviour of the BIIS in the North Sea. Using this framework, future efforts to  
871 date and model the ice sheet can more specifically target the climatic, mass-balance, and  
872 external glaciological factors (i.e. Fennoscandian Ice Sheet) that influenced deglaciation,  
873 important for better characterising both modern and palaeo-ice sheets.
- 874 • Lastly, this study provides an important demonstration of how improved bathymetry data  
875 and geomorphological interpretation over extensive areas enables the identification of  
876 greater detail within shallow seismic data, which in turn allows for more nuanced and  
877 accurate interpretations of ice sheet dynamics and relative event chronologies.

## 878 **Acknowledgements**

879 Bathymetry compilation contains public sector information from the Maritime and Coastguard  
880 Agency, and additional data from the UKHO Bathymetry Data Archive Centre, licensed under the  
881 Open Government Licence v2.0. Terrestrial topography data derived from Intermap Technologies  
882 NEXTMap Britain elevation data. Terrestrial glacial landforms and ice limits sourced from the BRITICE  
883 GIS database (Clark et al., 2004). Many thanks to Rhys Cooper for help in compiling the bathymetry  
884 data, and to Heather Stewart, Emrys Phillips, Carol Cotterill, Chris Clark, and Richard Chiverell for

885 useful discussions on the glaciation of the North Sea basin. Dayton Dove, Jonathan Lee, Dave Tappin,  
886 Claire Mellet, and Dave Long publish with the permission of the Executive Director, British Geological  
887 Survey (NERC). Dag Ottesen and Mark Batemen are thanked for constructive reviews, which helped  
888 to significantly improve the manuscript.

## 889 Figure Captions

- 890 1- North Sea bathymetry and study area. Gray lines show generalized LGM reconstruction of  
891 BISS and FIS extent and flow configuration (Graham et al., 2011). Three reconstructions of  
892 MIS 2 maximum are shown in white (contrasting line styles reflect different studies; see  
893 legend ). Contrasting reconstructions of later-stage glaciation (uncoupled BISS and FIS)  
894 shown in yellow (Carr et al., 2006) and blue (Sejrup et al., 2016). Terrestrial LGM limit in  
895 southern Britain taken from BRITICE (Clark et al., 2004). Source of bathymetry data:  
896 EMODnet. Northern MIS 2 margin adapted from Clark et al. (2012) and Bradwell and Stoker  
897 (2015).
- 898 2- Study area bathymetry with figure inset locations and feature names. Bathymetry data are  
899 compiled from the UK Bathymetry Data Archive Centre (DAC), and gridded to 25m horizontal  
900 resolution. Terrestrial topography: NEXTMap.
- 901 3- Oblique view, looking south down the Inner Silver Pit. The glacial tunnel valley exhibits  
902 significant vertical relief, exposes outcrops of deformed bedrock, and incorporates  
903 discontinuous Holocene sediment cover. High-resolution swath bathymetry from within the  
904 tunnel valley were acquired for the Silver Pit Marine Conservation Zone (MCZ), Defra, and  
905 made available under Open Government License Copyright.
- 906 4- Zoomed-in view of bathymetry, demonstrating glacial landform assemblage i.e relationship  
907 between till wedges, moraines, and tunnel valleys. Inset (top left) shows interpretation of  
908 glacial landforms.
- 909 5- Zoomed-in view of coast-parallel ridges offshore Holderness. These ridges may relate in part  
910 to the moraines mapped on Holderness (Evans and Thompson, 2010). These are shown  
911 within the bottom-left inset, together with newly-mapped offshore ridges. Swath  
912 bathymetry data were acquired by the Channel Coastal Observatory (CCO)-nearshore, and  
913 for recommended Marine Conservation Zones (MCZ)-offshore, Defra, and made available  
914 under Open Government License Copyright.
- 915 6- Revised seismostratigraphic model of the Bolders Bank Formation (blue fill). Panel A) shows  
916 seismic interpretation along our type section A-A'. Yellow fill indicates mobile and/or sand-  
917 rich deposit. Orange fill indicates mud-rich Holocene channel infill. Profile location shown in  
918 Fig. (2). Panel B) shows an extract of the seismic data highlighting key stratigraphic features  
919 that correspond to the seabed geomorphology (boomer; BGS survey 1990/4).
- 920 7- A) Seismic and B) interpreted sections along profile B-B', an offset boomer line from the  
921 southern end of profile A-A'. Seismic data reveal southern extent of buried wedge that is  
922 truncated on profile A-A', and the same seismostratigraphic nomenclature applies (i.e.  
923 seismic units I and II) as in Fig. 6.
- 924 8- A) Seismic and B) interpreted sections along profile C-C' (boomer data; BGS-held survey  
925 2008/5). Similar colour scheme used as along profiles A-A' and B-B' (Figs. 6,7) to  
926 demonstrate that similar seismic architectural patterns are observed across the study area  
927 (e.g. stacked till wedges). Seismostratigraphic units are not labelled however because it's not  
928 clear whether individual seismic sequences persist over large lateral distances (10's kms).
- 929 9- Interpreted glacial geomorphology of the study area. Observed glacial landforms used to  
930 infer approximate positions of four arcuate ice margins, numbered from south to north (1-  
931 4). White dots indicate the locations of BGS-held cores where Bolders Bank till was

932 recovered in shallow sediment cores (note that these do not persist south of Ice-margin  
 933 1). 'G.C.' indicates the location of the infilled Glacifluvial Channel on Fig. (6).  
 934 10- A) Regional extent (Bolders Bank Formation (BBF) and ice flow configuration (white arrows)  
 935 of the North Sea Lobe. Arcuate ice margins are projected away from observed landforms  
 936 and outwith the study area. These projected ice margins suggest good agreement with  
 937 previously observed terrestrial limits e.g. Ice-margin (I.M.) 1 and the LGM maximum in north  
 938 Norfolk (Clark et al., 2004), and moraine ridges in Lincolnshire and Holderness. Previously  
 939 mapped seismostratigraphic extent of the Bolders Bank Formation (BBF) superimposed on  
 940 regional hillshade bathymetry. B) Simplified conceptual diagram demonstrating the  
 941 relationships between the glacial landforms present at seabed (broad wedges, moraines,  
 942 tunnel valleys), and the revised stratigraphy of the BBF (shallow stacked till wedges). This  
 943 combined landform and sub-surface stratigraphic assemblage elucidates the phased still-  
 944 stand occupation of the North Sea Lobe at an oscillating southern margin, prior to final  
 945 retreat from the region .  
 946 11- Tunnel valley spacing vs. drainage (i.e. cross-sectional area). Regression analysis suggests a  
 947 proportional relationship between the lateral spacing and inferred discharge of the tunnel  
 948 valleys distributed along Ice-margin 4. This suggests that subglacial meltwater is strongly  
 949 focussed towards individual tunnel valleys, in which the size of the tunnel valley corresponds  
 950 to its broader catchment area.  
 951

## 952 **References:**

- 953  
 954 Agar, R., 1954. Glacial and post-glacial geology of Middlesbrough and the Tees Estuary. Proceedings  
 955 of the Yorkshire Geological Society, 29(3), pp.237-253.  
 956  
 957 Alley, R.B., Cuffey, K.M., Evenson, E.B., Strasser, J.C., Lawson, D.E. and Larson, G.J., 1997. How  
 958 glaciers entrain and transport basal sediment: Physical constraints. Quaternary Science  
 959 Reviews, 16(9), pp.1017-1038.  
 960  
 961 P.S. Balson, Jeffrey, D.H., 1991. The glacial sequence of the southern North Sea J. Ehlers, P.L.  
 962 Gibbard, J. Rose (Eds.), Glacial Deposits of Great Britain and Ireland, Balkema, Rotterdam (1991), pp.  
 963 245–253  
 964  
 965 Bateman, M.D., Buckland, P.C., Chase, B., Frederick, C.D. and Gaunt, G.D., 2008. The Late-Devensian  
 966 proglacial Lake Humber: new evidence from littoral deposits at Ferrybridge, Yorkshire,  
 967 England. Boreas, 37(2), pp.195-210.  
 968  
 969 Bateman, M.D., Buckland, P.C., Whyte, M.A., Ashurst, R.A., Boulter, C. and Panagiotakopulu, E.V.A.,  
 970 2011. Re-evaluation of the Last Glacial Maximum typesite at Dimlington, UK. Boreas, 40(4), pp.573-  
 971 584.  
 972  
 973 Bateman, M D, Evans, D J A, Buckland, P C, Connell, E R, Friend, R J, Hartmann, D, Moxon, H,  
 974 Fairburn, W A, Panagiotakopulu, E, AND Ashurst, R A. 2015. Last glacial dynamics of the Vale of York  
 975 and North Sea lobes of the British and Irish Ice Sheet. Proceedings of the Geologists' Association, Vol.  
 976 126, 712-730.  
 977  
 978 Böse, M., Lüthgens, C., Lee, J.R. and Rose, J., 2012. Quaternary glaciations of northern Europe.  
 979 Quaternary Science Reviews, 44, pp.1-25.  
 980  
 981 Boston, C M, Evans, D J A, AND Cofaigh, C Ó. 2010. Styles of till deposition at the margin of the Last  
 982 Glacial Maximum North Sea lobe of the British-Irish Ice Sheet: an assessment based on geochemical

983 properties of glacial deposits in eastern England. *Quaternary Science Reviews*, Vol. 29, 3184-  
 984 3211.  
 985  
 986 Boulton, G.S., Jones, A.S., Clayton, K.M. and Kenning, M.J., 1977. A British ice-sheet model and  
 987 patterns of glacial erosion and deposition in Britain. *British Quaternary Studies*, pp.231-246.  
 988  
 989 Boulton GS, Smith GD, Jones AS, Newsome J., 1985. Glacial geology and glaciology of the last mid-  
 990 latitude ice sheets. *Journal of the Geological Society*. 142(3):447-74.  
 991  
 992 Boulton, G.S., 1996a. Theory of glacial erosion, transport and deposition as a consequence of  
 993 subglacial sediment deformation. *Journal of Glaciology* 42, 43–62.  
  
 994 Boulton, G.S., 1996b. The origin of till sequences by subglacial sediment deformation beneath mid-  
 995 latitude ice sheets. *Annals of Glaciology* 22, 75–84.  
  
 996 Boulton, G.S., Dongelmans, P., Punkari, M. and Broadgate, M., 2001. Palaeoglaciology of an ice sheet  
 997 through a glacial cycle: the European ice sheet through the Weichselian. *Quaternary Science*  
 998 *Reviews*, 20(4), pp.591-625.  
 999  
 1000 Boulton, G.S., Hagdorn, M., Maillot, P.B. and Zatzepin, S., 2007. Drainage beneath ice sheets:  
 1001 groundwater–channel coupling, and the origin of esker systems from former ice sheets. *Quaternary*  
 1002 *Science Reviews*, 28(7), pp.621-638.  
 1003  
 1004 Boulton, G. and Hagdorn, M., 2006. Glaciology of the British Isles Ice Sheet during the last glacial  
 1005 cycle: form, flow, streams and lobes. *Quaternary Science Reviews*, 25(23), pp.3359-3390.  
 1006  
 1007 Bradwell, T., Stoker, M.S., Gollledge, N.R., Wilson, C.K., Merritt, J.W., Long, D., Everest, J.D., Hestvik,  
 1008 O.B., Stevenson, A.G., Hubbard, A.L. and Finlayson, A.G., 2008. The northern sector of the last British  
 1009 Ice Sheet: maximum extent and demise. *Earth-Science Reviews*, 88(3), pp.207-226.  
 1010  
 1011 Bradwell, T., Stoker, M.S., (2015). Asymmetric ice-sheet retreat pattern around Northern Scotland  
 1012 revealed by marine geophysical surveys. *Earth and Environmental Science Transactions of the Royal*  
 1013 *Society of Edinburgh*, 105: 297-322. DOI:10.1017/S1755691015000109.  
 1014  
 1015 Brand, D., Booth, S.J. and Rose, J., 2002. Late Devensian glaciation, ice-dammed lake and river  
 1016 diversion, Stiffkey, north Norfolk, England. *Proceedings of the Yorkshire Geological Society*, 54(1),  
 1017 pp.35-46.  
 1018  
 1019 British Geological Survey, 1991, 1:250 000 Series. Spurn: Quaternary Geology. British Geological  
 1020 Survey, Keyworth, Nottingham.  
 1021  
 1022 Busfield, M.E., Lee, J.R., Riding, J.B., Zalasiewicz, J. and Lee, S.V., 2015. Pleistocene till provenance in  
 1023 east Yorkshire: reconstructing ice flow of the British North Sea Lobe. *Proceedings of the Geologists'*  
 1024 *Association*, 126(1), pp.86-99.  
 1025  
 1026 Cameron, T.D.J., Stoker, M.S. and Long, D., 1987. The history of Quaternary sedimentation in the UK  
 1027 sector of the North Sea Basin. *Journal of the Geological Society*, 144(1), pp.43-58.  
 1028  
 1029 Cameron, T.D.J., Crosby, A., Balson, P.S., Jeffery, D.H., Lott, G.K., Bulat, J. and Harrison, D.J., 1992.  
 1030 The geology of the southern North Sea. United Kingdom offshore regional report. British Geological  
 1031 Survey and HMSO, London.

1032  
1033 Carr, S., 1999. The micromorphology of last glacial maximum sediments in the southern North  
1034 Sea. *Catena*, 35(2), pp.123-145.  
1035  
1036 Carr, S.J., Holmes, R.V.D., Van der Meer, J.J.M. and Rose, J., 2006. The Last Glacial Maximum in the  
1037 North Sea Basin: micromorphological evidence of extensive glaciation. *Journal of Quaternary*  
1038 *Science*, 21(2), pp.131-153.  
1039  
1040 Catt, J.A. and Penny, L.F., 1966. The Pleistocene deposits of Holderness, East Yorkshire. *Proceedings*  
1041 *of the Yorkshire Geological Society*, 35(3), pp.375-420.  
1042  
1043 Catt, J.A., 2007. The Pleistocene glaciations of eastern Yorkshire: a review. In *Proceedings of the*  
1044 *Yorkshire Geological and Polytechnic Society* (Vol. 56, No. 3, pp. 177-207). Geological Society of  
1045 London.  
1046  
1047 Clark, C.D., Hughes, A.L., Greenwood, S.L., Jordan, C. and Sejrup, H.P., 2012. Pattern and timing of  
1048 retreat of the last British-Irish Ice Sheet. *Quaternary Science Reviews*, 44, pp.112-146.  
1049  
1050 Cohen, K.M., Gibbard, P.L. and Weerts, H.J.T., 2014. North Sea palaeogeographical reconstructions  
1051 for the last 1 Ma. *Netherlands Journal of Geosciences-Geologie en Mijnbouw*, 93(1-2), pp.7-29.  
1052  
1053 Colgan, P.M., 1999. Reconstruction of the Green Bay lobe, Wisconsin, United States, from 26,000 to  
1054 13,000 radiocarbon years BP. *SPECIAL PAPERS-GEOLOGICAL SOCIETY OF AMERICA*, pp.137-150.  
1055  
1056 Colgan PM, Mickelson DM, Cutler PM, 2003. Ice-marginal terrestrial landsystems: southern  
1057 Laurentide Ice Sheet margin. *Glacial landsystems*. London: Arnold:111-42.  
1058  
1059 Cotterill, C.J., Long, D., James, L., Forsberg, C.F., Phillips, E., Tjelta, T.I., Dove, D., *In Prep*. The  
1060 evolution of the Dogger Bank, North Sea: a complex history of terrestrial, glacial and marine  
1061 environmental change.  
1062  
1063 Davies, B.J., Roberts, D.H., Ó COFAIGH, C.O.L.M., Bridgland, D.R., Riding, J.B., Phillips, E.R. and  
1064 Teasdale, D.A., 2009. Interlobate ice-sheet dynamics during the Last Glacial Maximum at Whitburn  
1065 Bay, County Durham, England. *Boreas*, 38(3), pp.555-578.  
1066  
1067 Davies, B.J., Roberts, D.H., Bridgland, D.R., Cofaigh, C.Ó. and Riding, J.B., 2011. Provenance and  
1068 depositional environments of Quaternary sediments from the western North Sea Basin. *Journal of*  
1069 *Quaternary Science*, 26(1), pp.59-75.  
1070  
1071 DeConto, R.M. and Pollard, D., 2016. Contribution of Antarctica to past and future sea-level rise.  
1072 *Nature*, 531(7596), pp.591-597  
1073  
1074 Donovan, D. T. "The geology and origin of the Silver Pit and other closed basins in the North Sea."  
1075 In *Proceedings of the Yorkshire Geological and Polytechnic Society*, vol. 39, no. 2, pp. 267-293.  
1076 Geological Society of London, 1972.  
1077  
1078 Dove, D., Arosio, R., Finlayson, A., Bradwell, T. and Howe, J.A., 2015. Submarine glacial landforms  
1079 record Late Pleistocene ice-sheet dynamics, Inner Hebrides, Scotland. *Quaternary Science*  
1080 *Reviews*, 123, pp.76-90.  
1081

1082 Dowdeswell, J.A., Ottesen, D., Evans, J., Cofaigh, C.Ó. and Anderson, J.B., 2008. Submarine glacial  
1083 landforms and rates of ice-stream collapse. *Geology*, 36(10), pp.819-822.

1084

1085 Dowdeswell, J.A. and Ottesen, D., 2013. Buried iceberg ploughmarks in the early Quaternary  
1086 sediments of the central North Sea: a two-million year record of glacial influence from 3D seismic  
1087 data. *Marine Geology*, 344, pp.1-9.

1088

1089 Dowdeswell JA, Hogan KA, Arnold NS, Mugford RI, Wells M, Hirst JP, Decalf C. Sediment-rich  
1090 meltwater plumes and ice-proximal fans at the margins of modern and ancient tidewater glaciers:  
1091 Observations and modelling. *Sedimentology*. 2015 Oct 1;62(6):1665-92.

1092

1093 Ekman, S.R., 1998. Pleistocene pollen stratigraphy from borehole 81/34, Devil's hole area, central  
1094 North Sea. *Quaternary science reviews*, 17(9), pp.855-869.

1095

1096 Ehlers, J., Meyer, K.D. and Stephan, H.J., 1984. The pre-Weichselian glaciations of north-west  
1097 Europe. *Quaternary Science Reviews*, 3(1), pp.111-940.

1098

1099 Ehlers, J. and Wingfield, R., 1991. The extension of the late Weichselian/late Devensian ice sheets in  
1100 the North Sea basin. *Journal of Quaternary Science*, 6(4), pp.313-326

1101

1102 England, A C, and Lee, J A. 1991. Quaternary deposits of the eastern Wash Margin. *Bulletin of the*  
1103 *Geological Society of Norfolk*, Vol. 40, 67-99.

1104

1105 Evans, D J A, Owen, L A, and Roberts, D. 1995. Stratigraphy and sedimentology of Devensian  
1106 (Dimlington Stadial) glacial deposits, east Yorkshire, England. *Journal of Quaternary Science*, Vol. 10,  
1107 241-265.

1108

1109 Evans, D.J. and Twigg, D.R., 2002. The active temperate glacial landsystem: a model based on  
1110 Breiðamerkurjökull and Fjallsjökull, Iceland. *Quaternary science reviews*, 21(20), pp.2143-2177.

1111

1112 Evans, D.J. and Hiemstra, J.F., 2005. Till deposition by glacier submarginal, incremental thickening.  
1113 *Earth Surface Processes and Landforms*, 30(13), pp.1633-1662.

1114

1115 Evans, D.J.A., Phillips, E.R., Hiemstra, J.F. and Auton, C.A., 2006. Subglacial till: formation,  
1116 sedimentary characteristics and classification. *Earth-Science Reviews*, 78(1), pp.115-176.

1117

1118 Evans, D.J., Clark, C.D. and Rea, B.R., 2008. Landform and sediment imprints of fast glacier flow in  
1119 the southwest Laurentide Ice Sheet. *Journal of Quaternary Science*, 23(3), pp.249-272.

1120

1121 Evans, D.J. and Thomson, S.A., 2010. Glacial sediments and landforms of Holderness, eastern  
1122 England: a glacial depositional model for the North Sea Lobe of the British-Irish Ice Sheet. *Earth-*  
1123 *Science Reviews*, 101(3), pp.147-189.

1124

1125 Evans, D.J., Hiemstra, J.F., Boston, C.M., Leighton, I., Cofaigh, C.Ó. and Rea, B.R., 2012. Till  
1126 stratigraphy and sedimentology at the margins of terrestrially terminating ice streams: case study of  
1127 the western Canadian prairies and high plains. *Quaternary Science Reviews*, 46, pp.80-125.

1128

1129 Evans, D.J., Young, N.J. and Cofaigh, C.Ó., 2014. Glacial geomorphology of terrestrial-terminating fast  
1130 flow lobes/ice stream margins in the southwest Laurentide Ice Sheet. *Geomorphology*, 204, pp.86-  
1131 113.

1132

1133 Evans, D.J., Ewertowski, M. and Orton, C., 2015. Fláajökull (north lobe), Iceland: active temperate  
1134 piedmont lobe glacial landsystem. *Journal of Maps*, pp.1-13.

1135

1136 Evans DJ, Bateman MD, Roberts DH, Medialdea A, Hayes L, Duller GA, Fabel D, Clark CD. Glacial Lake  
1137 Pickering: stratigraphy and chronology of a proglacial lake dammed by the North Sea Lobe of the  
1138 British-Irish Ice Sheet, 2016. *Journal of Quaternary Science*. DOI: 10.1002/jqs.2833

1139

1140 Eyles, N., McCabe, A.M. and Bowen, D.Q., 1994. The stratigraphic and sedimentological significance  
1141 of Late Devensian ice sheet surging in Holderness, Yorkshire, UK. *Quaternary Science Reviews*, 13(8),  
1142 pp.727-759.

1143

1144 Eyles, N., Eyles, C., Menzies, J. and Boyce, J., 2011. End moraine construction by incremental till  
1145 deposition below the Laurentide Ice Sheet: Southern Ontario, Canada. *Boreas*, 40(1), pp.92-104.

1146

1147

1148 Fannin, N.G.T. 1989. Offshore investigations 1966-87. British Geological Survey Technical Report  
1149 WB/89/2.

1150

1151 Fairburn, W.A. and Bateman, M.D., 2016. A new multi-stage recession model for Proglacial Lake  
1152 Humber during the retreat of the last British-Irish Ice Sheet. *Boreas*, 45(1), pp.133-151.

1153

1154 Fitch, S., Thomson, K. and Gaffney, V., 2005. Late Pleistocene and Holocene depositional systems  
1155 and the palaeogeography of the Dogger Bank, North Sea. *Quaternary Research*, 64(2), pp.185-196.

1156

1157 Gaffney, V.L., Thomson, K. and Fitch, S., 2007. Mapping Doggerland: the Mesolithic landscapes of the  
1158 southern North Sea. *Archaeopress*.

1159

1160 Gallois, R. W. 1994. The geology of the country around King's Lynn and The Wash. Memoir of the  
1161 British Geological Survey, sheet 145 and part of 129 (England and Wales).

1162

1163 Gatliff, R.W., Richards, P.C., Smith, K., Graham, C.C., McCormac, M., Smith, N.J.P., Long, D., Cameron,  
1164 T.D.J., Evans, D., Stevenson, A.G. and Bulat, J., 1994. United Kingdom offshore regional report: the  
1165 geology of the central North Sea. HSMO, London.

1166

1167 Graham, Alastair G.C.; Stoker, Martyn S.; Lonergan, Lidia; Bradwell, Tom; Stewart, Margaret A.. 2011  
1168 The Pleistocene glaciations of the North Sea Basin. In: Ehlers, J.; Gibbard, P.L.; Hughes, P.D., (eds.)  
1169 Quaternary glaciations : extent and chronology : a closer look. Elsevier, 261-278. (Developments in  
1170 Quaternary Science, 15).

1171

1172 Harrison, D.J., 1992. The marine sand and gravel resources off the Humber. British Geological Survey  
1173 Technical Report WB/92/1.

1174

1175 Hewitt, I.J., 2011. Modelling distributed and channelized subglacial drainage: the spacing of  
1176 channels. *Journal of Glaciology*, 57(202), pp.302-314.

1177

1178 Hooke, R.L. and Fastook, J., 2007. Thermal conditions at the bed of the Laurentide ice sheet in Maine  
1179 during deglaciation: implications for esker formation. *Journal of Glaciology*, 53(183), pp.646-658.

1180

1181 Houmark-Nielsen, M., 2007. Extent and age of Middle and Late Pleistocene glaciations and  
1182 periglacial episodes in southern Jylland, Denmark. *Bulletin of the Geological Society of Denmark*,  
1183 55(1), pp.9-35.

1184  
1185 Houmark-Nielsen, M., 2011. Pleistocene glaciations in Denmark: a closer look at chronology, ice  
1186 dynamics and landforms. *Developments in Quaternary Science*, 15, pp.47-58.  
1187  
1188 Hubbard, A., Bradwell, T., Golledge, N., Hall, A., Patton, H., Sugden, D., Cooper, R. and Stoker, M.,  
1189 2009. Dynamic cycles, ice streams and their impact on the extent, chronology and deglaciation of the  
1190 British-Irish ice sheet. *Quaternary Science Reviews*, 28(7), pp.758-776.  
1191  
1192 Hughes, A.L., Gyllencreutz, R., Lohne, Ø.S., Mangerud, J. and Svendsen, J.I., 2016. The last Eurasian  
1193 ice sheets—a chronological database and time-slice reconstruction, DATED-1. *Boreas*, 45(1), pp.1-45.  
1194  
1195 Huuse M, Lykke-Andersen H, 2000. Overdeepened Quaternary valleys in the eastern Danish North  
1196 Sea: morphology and origin. *Quaternary Science Reviews*. 19(12):1233-53.  
1197  
1198 Jansen, J.H.F., Van Weering, T.C. and Eisma, D., 1979. Late Quaternary sedimentation in the North  
1199 Sea. In *The quaternary history of the North Sea. Acta Universitatis, Symposium Universitatis*  
1200 *Usaliensis Annum Quingentesimum Celebrantis* (pp. 175-187).  
1201  
1202 Jennings, C.E., 2006. Terrestrial ice streams—a view from the lobe. *Geomorphology*, 75(1), pp.100-  
1203 124.  
1204  
1205 Jørgensen, F. and Sandersen, P.B., 2006. Buried and open tunnel valleys in Denmark—erosion  
1206 beneath multiple ice sheets. *Quaternary Science Reviews*, 25(11), pp.1339-1363.  
1207  
1208 Kalm, V., 2012. Ice-flow pattern and extent of the last Scandinavian Ice Sheet southeast of the Baltic  
1209 Sea. *Quaternary Science Reviews*, 44, pp.51-59.  
1210  
1211 Kehew, A.E., Piotrowski, J.A., and Jørgensen, F., 2012. Tunnel valleys: Concepts and controversies—A  
1212 review." *Earth-Science Reviews* 113, no. 1, 33-58.  
1213  
1214 Kendall P.F. 1902. A system of glacier-lakes in the Cleveland Hills. *Quarterly Journal of the Geological*  
1215 *Society* 58: 471–571 [DOI: 10.1144/GSL.JGS.1902.058.01-04.32].  
1216  
1217 Laban, C., 1995. The Pleistocene glaciations in the Dutch sector of the North Sea. A synthesis of  
1218 sedimentary and seismic data. Ph.D. Thesis, University of Amsterdam.  
1219  
1220 Laban, C. and van der Meer, J.J., 2011. Pleistocene glaciation in the Netherlands. *Quaternary*  
1221 *Glaciations—Extent and Chronology—a closer look. Developments in Quaternary Science*, 15, pp.247-  
1222 260.  
1223  
1224 Lee, J.R., Rose, J., Hamblin, R.J., Moorlock, B.S., Riding, J.B., Phillips, E., Barendregt, R.W. and Candy,  
1225 I., 2011. The Glacial History of the British Isles during the Early and Middle Pleistocene: Implications  
1226 for the long-term development of the British Ice Sheet. *Quaternary Glaciations—Extent and*  
1227 *Chronology, A Closer Look. Developments in Quaternary Science. Elsevier, Amsterdam*, pp.59-74.  
1228  
1229 Lee, J.R., Phillips, E., Rose, J. and Vaughan-Hirsch, D., 2016. The Middle Pleistocene glacial evolution  
1230 of northern East Anglia, UK: a dynamic tectonostratigraphic–parasequence approach. *Journal of*  
1231 *Quaternary Science*.  
1232  
1233 Leysinger Vieli, G.J. and Gudmundsson, G.H., 2010. A numerical study of glacier advance over  
1234 deforming till. *The cryosphere.*, 4(3), pp.359-372.

1235  
1236 Livingstone, S.J., Evans, D.J., Cofaigh, C.Ó., Davies, B.J., Merritt, J.W., Huddart, D., Mitchell, W.A.,  
1237 Roberts, D.H. and Yorke, L., 2012. Glaciodynamics of the central sector of the last British-Irish Ice  
1238 Sheet in Northern England. *Earth-Science Reviews*, 111(1), pp.25-55.  
1239  
1240 Long, D., C. Laban, H. Streif, T. D. J. Cameron, R. T. E. Schuttenhelm, and R. Paepe. "The Sedimentary  
1241 Record of Climatic Variation in the Southern North Sea [and Discussion]." *Philosophical Transactions*  
1242 *of the Royal Society of London B: Biological Sciences* 318, no. 1191 (1988): 523-537.  
1243  
1244 Madgett, P.A. and Catt, J.A., 1978, March. Petrography, stratigraphy and weathering of Late  
1245 Pleistocene tills in East Yorkshire, Lincolnshire and north Norfolk. In *Proceedings of the Yorkshire*  
1246 *Geological and Polytechnic Society* (Vol. 42, No. 1, pp. 55-108). Geological Society of London.  
1247  
1248 Moorlock, B S P, Booth, S J, Hamblin, R J O, Pawley, S J, Smith, N J P, AND Woods, M A. 2008.  
1249 *Geology of the Wells-next-the-Sea district - a brief explanation of the geological map. Sheet*  
1250 *Explanation of the British Geological Survey. 1:50 000 Sheet 130 (England and Wales).*  
1251  
1252 Moreau, J., Huuse, M., Janszen, A., Van Der Vegt, P., Gibbard, P.L. and Moscarriello, A., 2012. The  
1253 glaciogenic unconformity of the southern North Sea. *Geological Society, London, Special*  
1254 *Publications*, 368(1), pp.99-110.  
1255  
1256 Moreau, J. and Huuse, M., 2014. Infill of tunnel valleys associated with landward-flowing ice sheets:  
1257 The missing Middle Pleistocene record of the NW European rivers?. *Geochemistry, Geophysics,*  
1258 *Geosystems*, 15(1), pp.1-9.  
1259  
1260 Mortimore, R. and James, L., 2015. The search for onshore analogues for the offshore Upper  
1261 Cretaceous Chalk of the North Sea. *Proceedings of the Geologists' Association*, 126(2), pp.188-210.  
1262  
1263 Ó Cofaigh, C.O., Dowdswell, J.A., Allen, C.S., Hiemstra, J.F., Pudsey, C.J., Evans, J.,  
1264 Evans, D.J.A., 2005. Flow dynamics and till genesis associated with a marinebased  
1265 Antarctic paleo-ice stream. *Quaternary Science Reviews* 24, 709-740.  
1266  
1267 Cofaigh, C.Ó., Evans, D.J. and Smith, I.R., 2010. Large-scale reorganization and sedimentation of  
1268 terrestrial ice streams during late Wisconsinan Laurentide Ice Sheet deglaciation. *Geological Society*  
1269 *of America Bulletin*, 122(5-6), pp.743-756.  
1270  
1271 Pawley, S M, Candy, I, AND Booth, S J. 2006. The Late Devensian terminal moraine ridge at Garrett  
1272 Hill, Stiffkey valley, north Norfolk, England. *Proceedings of the Yorkshire Geological Society*, Vol. 56,  
1273 31-39.  
1274  
1275 Patterson, C.J., 1997. Southern Laurentide ice lobes were created by ice streams: Des Moines Lobe in  
1276 Minnesota, USA. *Sedimentary Geology*, 111(1), pp.249-261.  
1277  
1278 Patterson, C.J., 1998. Laurentide glacial landscapes: The role of ice streams. *Geology*, 26(7), pp.643-  
1279 646.  
1280  
1281 Penny, L.F., Coope, G.R. and Catt, J.A., 1969. Age and insect fauna of the Dimlington Silts, East  
1282 Yorkshire.  
1283  
1284 Plater, A.J., Ridgway, J., Rayner, B., Shennan, I., Horton, B.P., Haworth, E.Y., Wright, M.R.,  
1285 Rutherford, M.M. and Wintle, A.G., 2000. Sediment provenance and flux in the Tees Estuary: the

1286 record from the Late Devensian to the present. Geological Society, London, Special  
1287 Publications, 166(1), pp.171-195.

1288

1289 Praeg, D., 2003. Seismic imaging of mid-Pleistocene tunnel-valleys in the North Sea Basin—high  
1290 resolution from low frequencies. *Journal of Applied Geophysics*, 53(4), pp.273-298.

1291

1292 Price, R.J., 1970. Moraines at Fjallsjökull, Iceland. *Arctic and Alpine Research*, pp.27-42.

1293

1294 Pringle, A.W., 1985. Holderness coast erosion and the significance of ords. *Earth Surface Processes  
1295 and Landforms*, 10(2), pp.107-124.

1296

1297 ROBERTS, D H, EVANS, D J A, LODWICK, J, AND COX, N J. 2013. The subglacial and ice-marginal  
1298 signature of the North Sea Lobe of the British–Irish Ice Sheet during the  
1299 Roberts, D H, Evans, D J A, Lodwick, J, AND Cox, N J. 2013. The subglacial and ice-marginal signature  
1300 of the North Sea Lobe of the British–Irish Ice Sheet during the Last Glacial Maximum at Upgang,  
1301 North Yorkshire, UK. *Proceedings of the Geologists' Association*, Vol. 124, 503-519.

1302

1303 Roberts, D.H., Evans, D.J.A., Callard, L., Dove, D., Bateman, M.D., Medialdea, A., Saher, M., Ó Cofaigh,  
1304 C., Chiverrell, R., Moreton S.G., Cotterill, C., Clark, C.D, In Prep. The MIS II limit of the British-Irish Ice  
1305 Sheet in the southern North Sea.

1306

1307 Rose, J., 1985. The Dimlington Stadial/Dimlington Chronozone: a proposal for naming the main  
1308 glacial episode of the Late Devensian in Britain. *Boreas*, 14(3), pp.225-230.

1309

1310 Scourse, J.D., Haapaniemi, A.I., Colmenero-Hidalgo, E., Peck, V.L., Hall, I.R., Austin, W.E., Knutz, P.C.  
1311 and Zahn, R., 2009. Growth, dynamics and deglaciation of the last British–Irish ice sheet: the deep-  
1312 sea ice-rafted detritus record. *Quaternary Science Reviews*, 28(27), pp.3066-3084.

1313

1314 Sejrup, H.P., Hafliðason, H., Aarseth, I., King, E., Forsberg, C.F., Long, D. and Rokoengen, K., 1994.  
1315 Late Weichselian glaciation history of the northern North Sea. *Boreas-International Journal of  
1316 Quaternary Research*, 23(1), pp.1-13.

1317

1318 Sejrup, H.P., Larsen, E., Landvik, J., King, E.L., Hafliðason, H. and Nesje, A., 2000. Quaternary  
1319 glaciations in southern Fennoscandia: evidence from southwestern Norway and the northern North  
1320 Sea region. *Quaternary Science Reviews*, 19(7), pp.667-685.

1321

1322 Sejrup, H.P., Nygård, A., Hall, A.M. and Hafliðason, H., 2009. Middle and Late Weichselian  
1323 (Devensian) glaciation history of south-western Norway, North Sea and eastern UK. *Quaternary  
1324 Science Reviews*, 28(3), pp.370-380.

1325

1326 Sejrup, H.P., Clark, C.D. and Hjelstuen, B.O., 2016. Rapid ice sheet retreat triggered by ice stream  
1327 debuitressing: Evidence from the North Sea. *Geology*, 44(5), pp.355-358.

1328

1329 Smith, D.B. 1981. The Quaternary geology of the Sunderland district, north-east England. In *The  
1330 Quaternary in Britain*, Neale J, Flenley J (eds). Pergamon: Oxford; 146–167.

1331

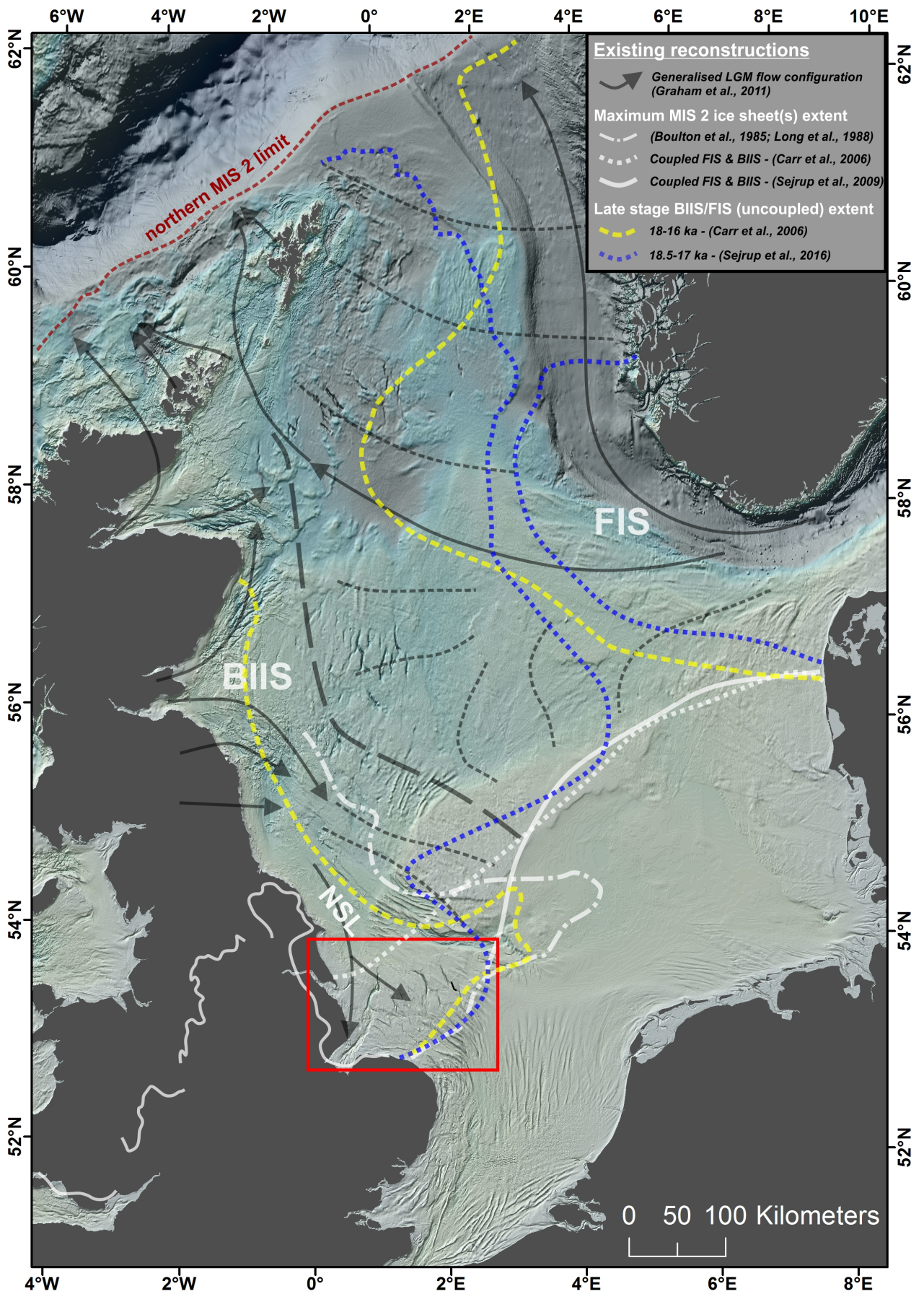
1332 Smith, D.B., 1994. *Geology of the country around Sunderland*. HMSO, London.

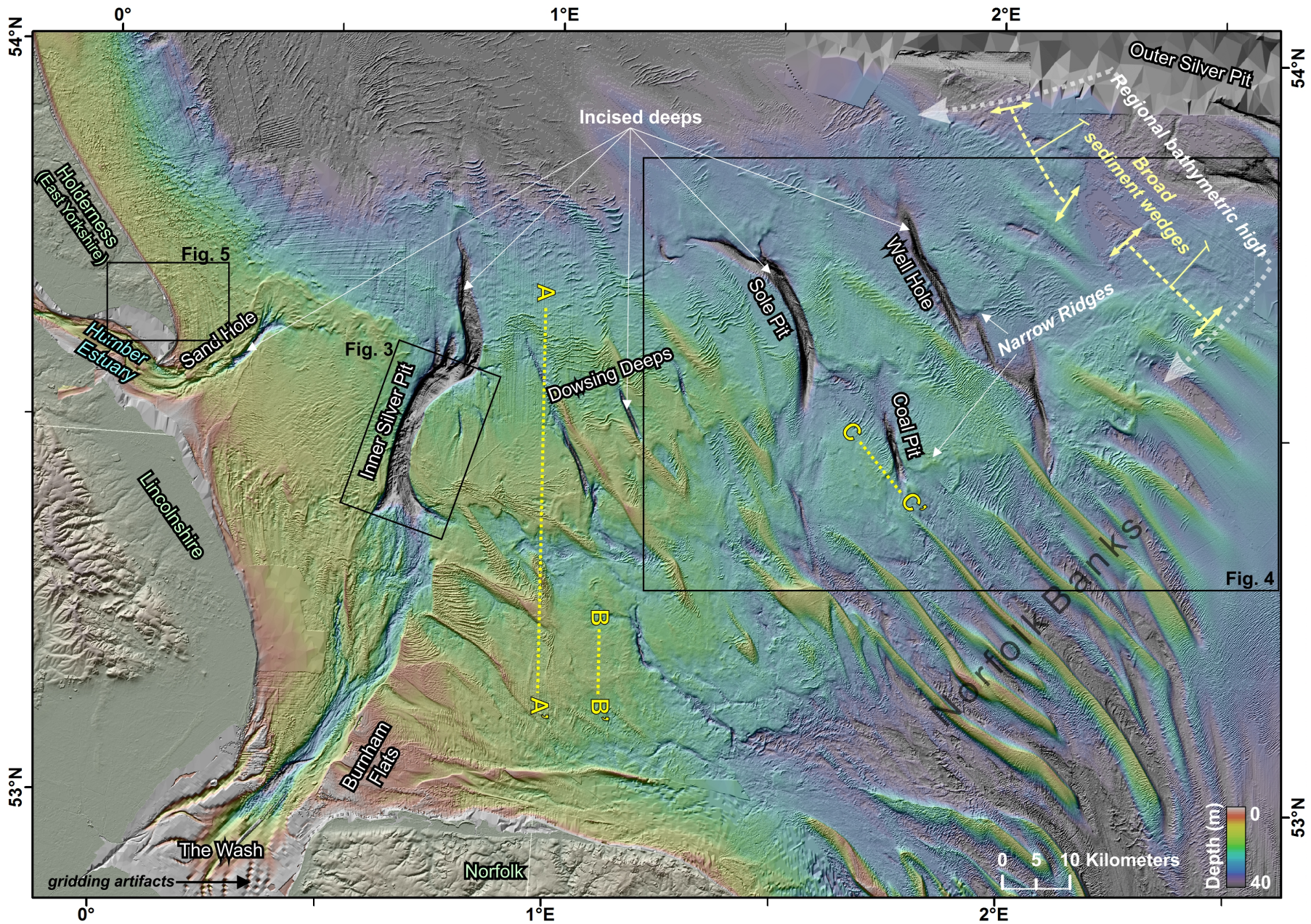
1333

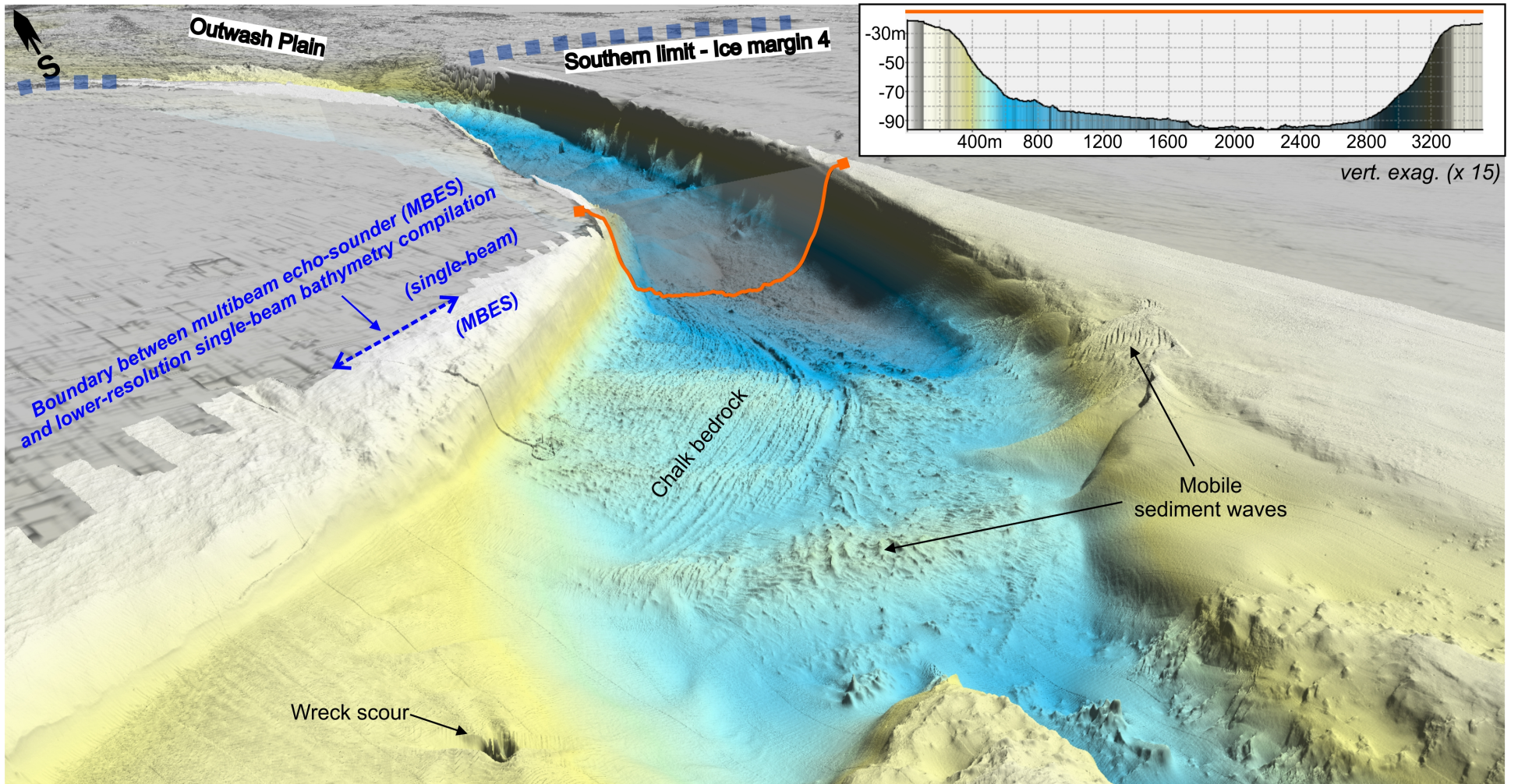
1334 Stewart, F.S., Stoker, M.S., 1990. Problems associated with seismic facies analysis of  
1335 diamicton-dominated, shelf glacial sequences. *Geo-Marine Letters* 10, 151e  
1336 156.

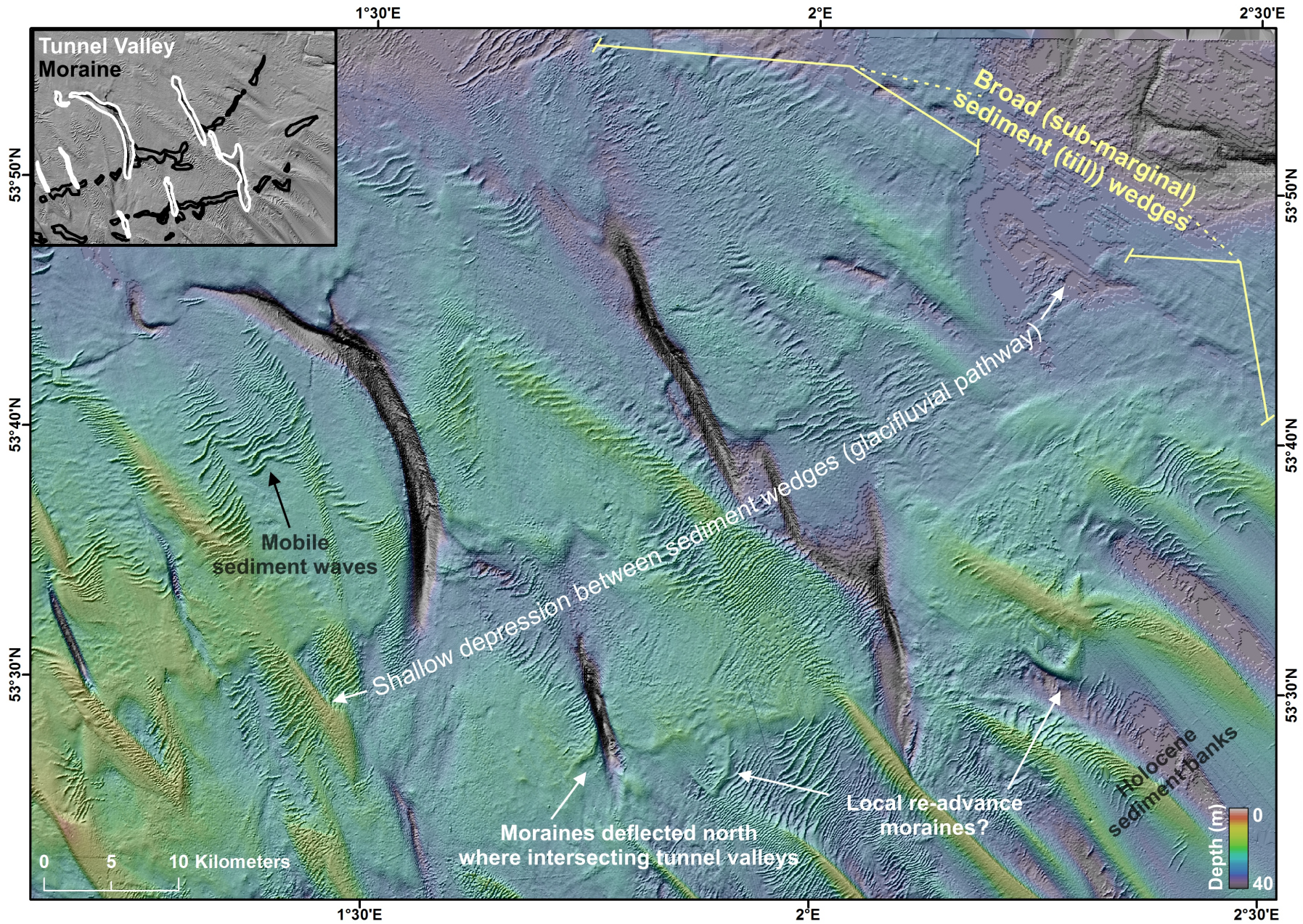
1337  
1338 Stewart, M.A. and Lonergan, L., 2011. Seven glacial cycles in the middle-late Pleistocene of  
1339 northwest Europe: Geomorphic evidence from buried tunnel valleys. *Geology*, 39(3), pp.283-286.  
1340  
1341 Stoker MS, Balson PS, Long D, Tappin DR. 2011. An overview of the lithostratigraphical framework  
1342 for the Quaternary deposits on the United Kingdom continental shelf. British Geological Survey  
1343 Research Report RR/11/03.  
1344  
1345 Stokes, C.R. and Clark, C.D., 2001. Palaeo-ice streams. *Quaternary Science Reviews*, 20(13), pp.1437-  
1346 1457.  
1347  
1348 Storrar, R.D., Stokes, C.R. and Evans, D.J., 2014. Morphometry and pattern of a large sample (>  
1349 20,000) of Canadian eskers and implications for subglacial drainage beneath ice sheets. *Quaternary*  
1350 *Science Reviews*, 105, pp.1-25.  
1351  
1352 Sturt, F., Garrow, D. and Bradley, S., 2013. New models of North West European Holocene  
1353 palaeogeography and inundation. *Journal of Archaeological Science*, 40(11), pp.3963-3976.  
1354  
1355 Tappin, D.R., Pearce, B., Fitch, S., Dove, D., Gearey, B., Hill, J.M., Chambers, C., Bates, R., Pinnion, J.,  
1356 Diaz Doce, D. and Green, M., 2011. The Humber regional environmental characterisation. Marine  
1357 Aggregate Levy Sustainability Fund.  
1358  
1359 Teasdale, D., Hughes, D., 1999. The glacial history of north-east England. In: Bridgland, D.R., Horton,  
1360 B.P., Innes, J.B. (Eds.), *The Quaternary of North East England: Field Guide*. Quaternary Research  
1361 Association, London, pp. 10- 17.  
1362  
1363 Todd, B.J., Valentine, P.C., Longva, O. and Shaw, J., 2007. Glacial landforms on German Bank, Scotian  
1364 Shelf: evidence for Late Wisconsinan ice-sheet dynamics and implications for the formation of De  
1365 Geer moraines. *Boreas*, 36(2), pp.148-169.  
1366  
1367 Toucanne, S., Zaragosi, S., Bourillet, J.F., Marieu, V., Cremer, M., Kageyama, M., Van Vliet-Lanoë, B.,  
1368 Eynaud, F., Turon, J.L. and Gibbard, P.L., 2010. The first estimation of Fleuve Manche palaeoriver  
1369 discharge during the last deglaciation: evidence for Fennoscandian ice sheet meltwater flow in the  
1370 English Channel ca 20–18ka ago. *Earth and Planetary Science Letters*, 290(3), pp.459-473.  
1371  
1372 Uehara, K., Scourse, J.D., Horsburgh, K.J., Lambeck, K. and Purcell, A.P., 2006. Tidal evolution of the  
1373 northwest European shelf seas from the Last Glacial Maximum to the present. *Journal of*  
1374 *Geophysical Research: Oceans*, 111(C9).  
1375  
1376 Valentin, H., 1957. Glazialmorphologische Untersuchungen in Ostengland: ein Beitrag zum Problem  
1377 der letzten Vereisung im Nordseeraum. Reimer.  
1378  
1379 Van der Vegt, P., Janszen, A. and Moscariello, A., 2012. Tunnel valleys: current knowledge and future  
1380 perspectives. Geological Society, London, Special Publications, 368(1), pp.75-97.  
1381  
1382 Veenstra, H.J., 1965. Geology of the Dogger Bank area, North Sea. *Marine Geology*, 3(4), pp.245-262.  
1383  
1384 Ward, S.L., Neill, S.P., Scourse, J.D., Bradley, S.L. and Uehara, K., 2016. Sensitivity of palaeotidal  
1385 models of the northwest European shelf seas to glacial isostatic adjustment since the Last Glacial  
1386 Maximum. *Quaternary Science Reviews*, 151, pp.198-211.  
1387

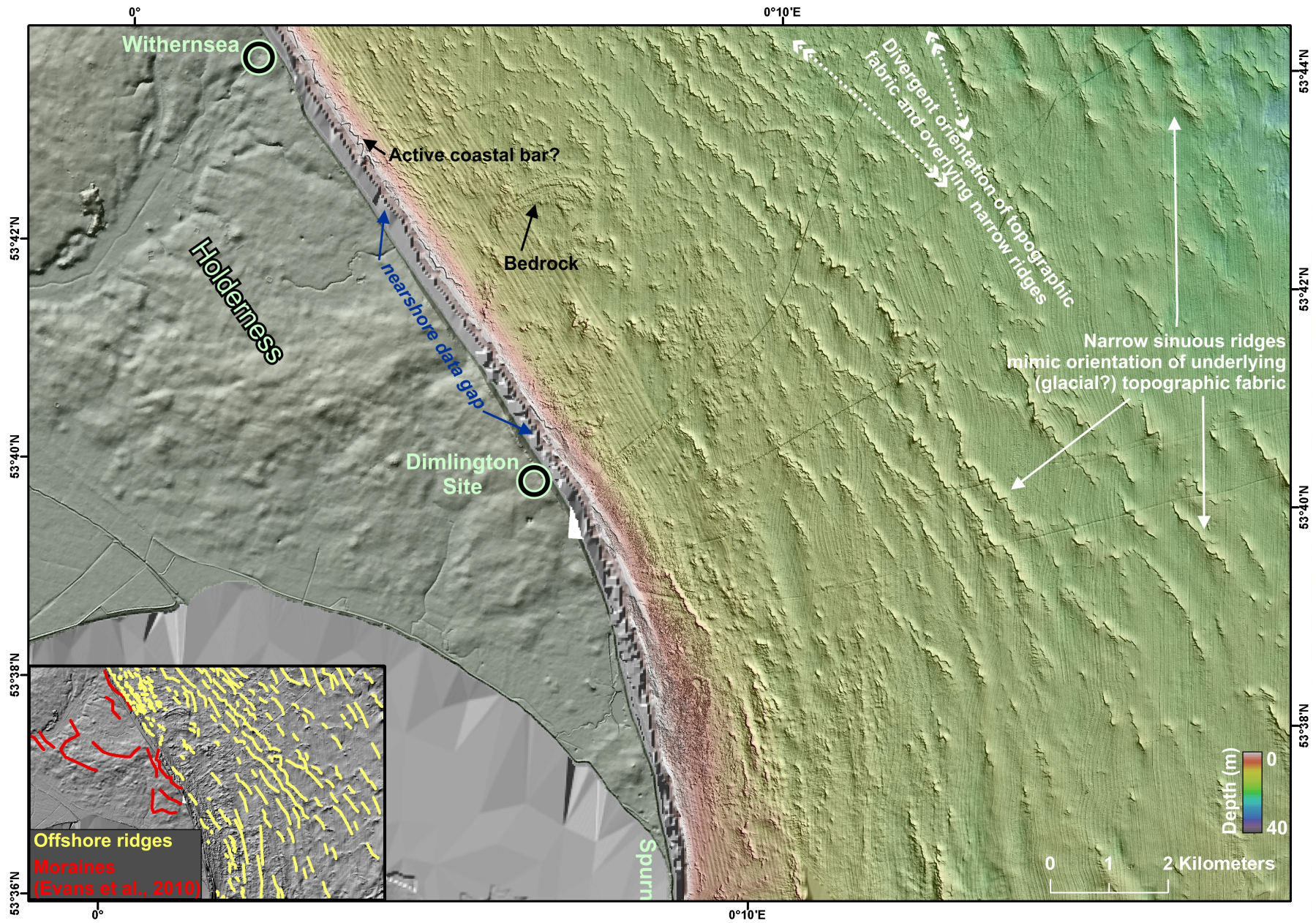
1388 Wingfield, R., 1990.. The origin of major incisions within the Pleistocene deposits of the North  
1389 Sea. Marine Geology 91, no. 1: 31-52.

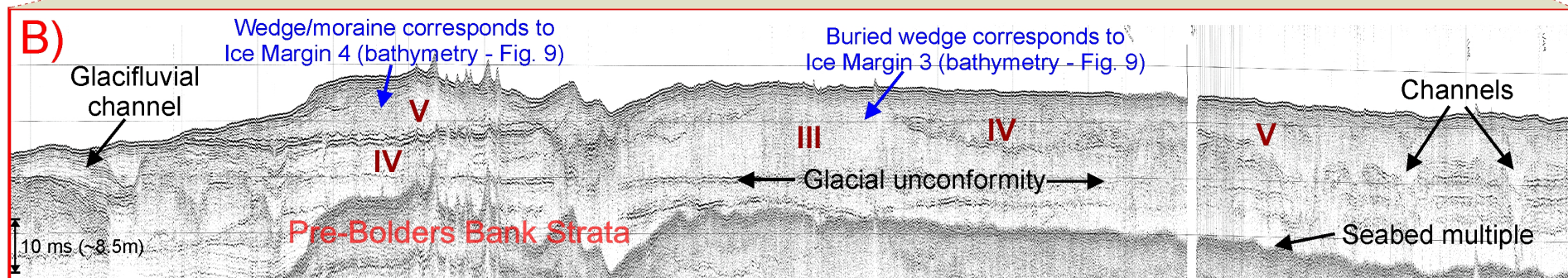
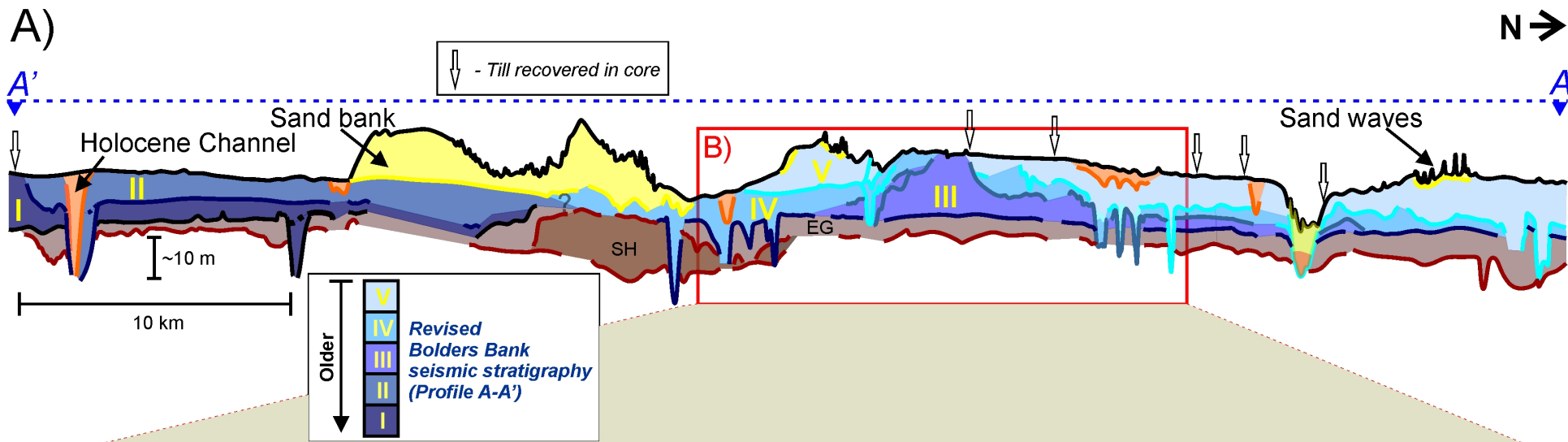




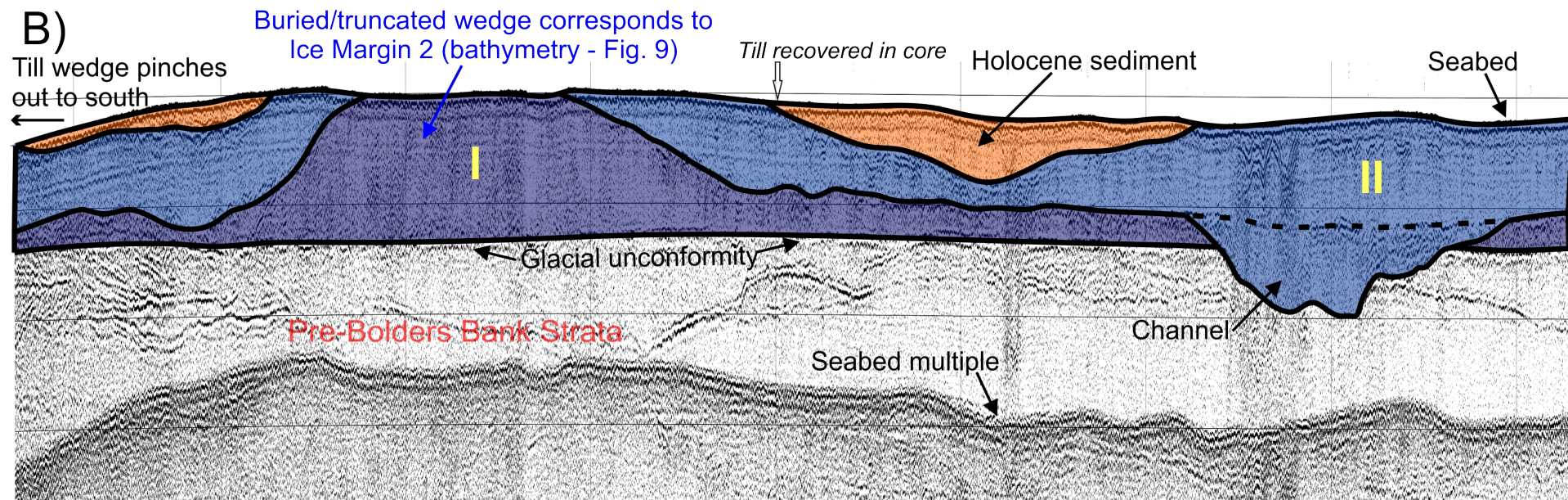
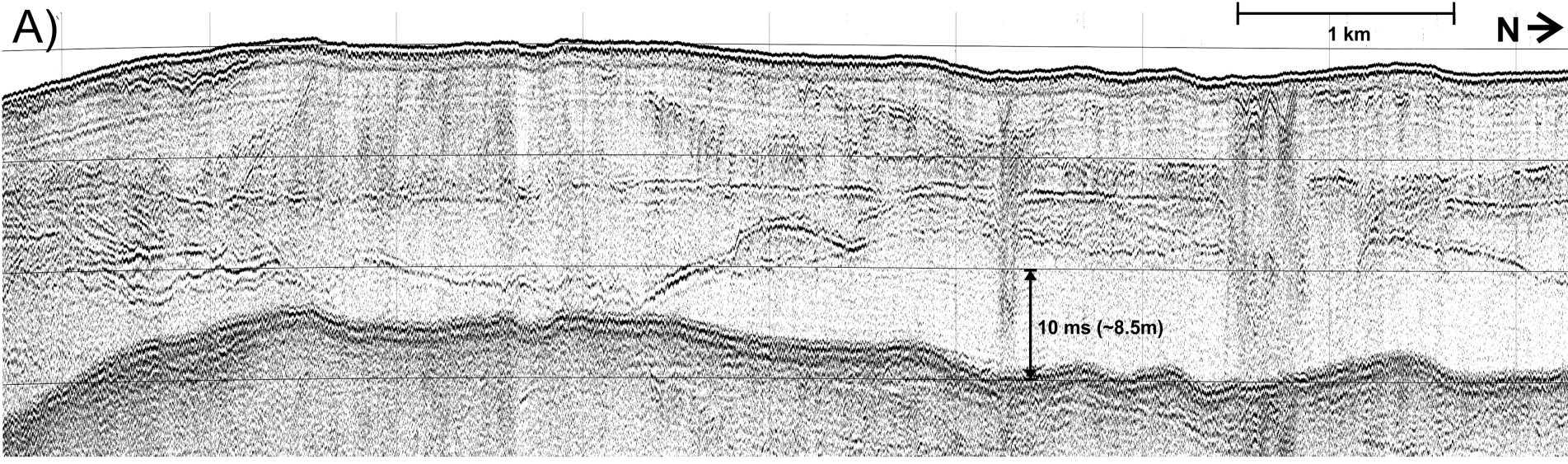




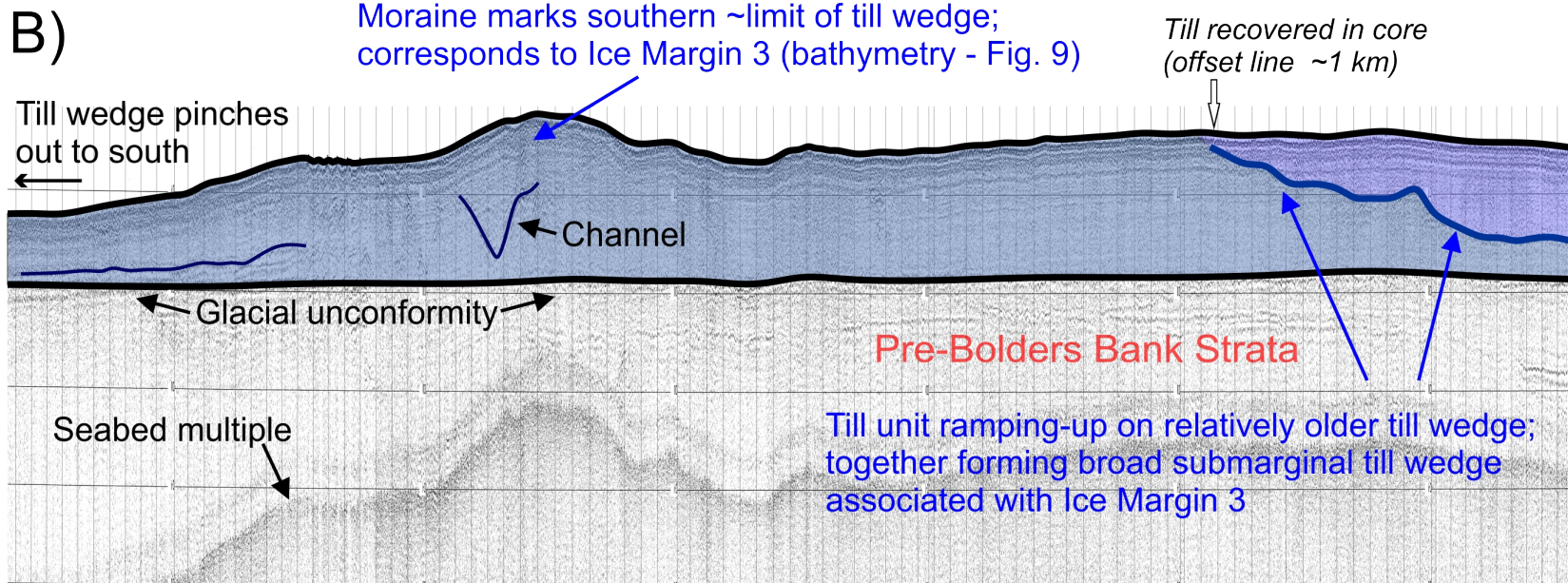
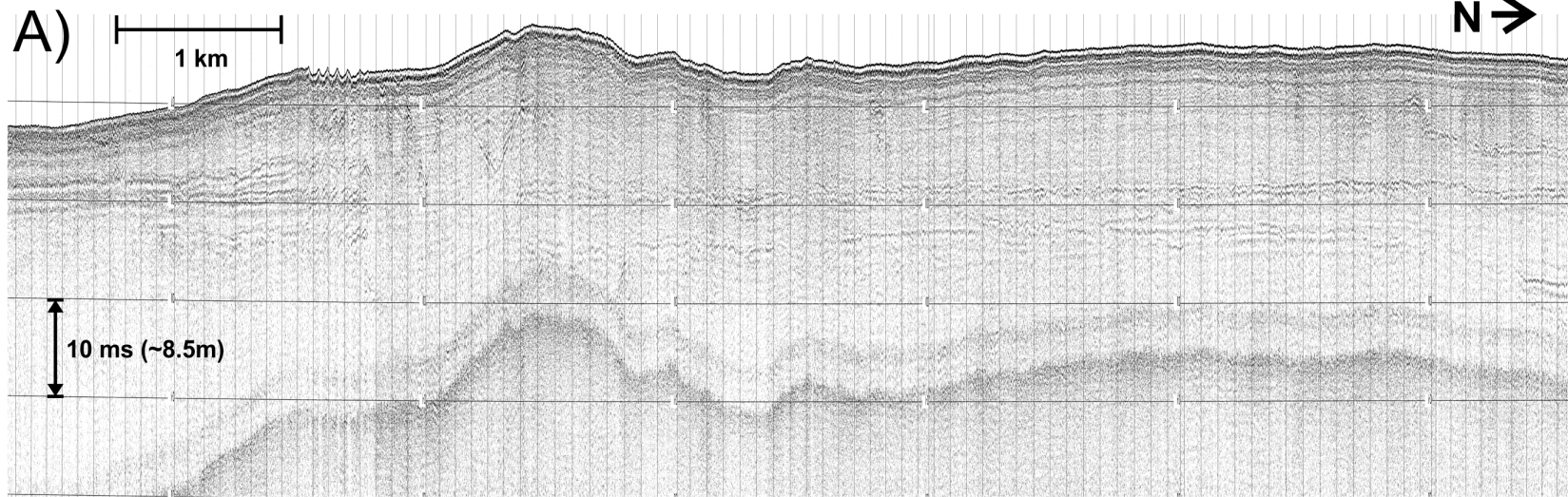


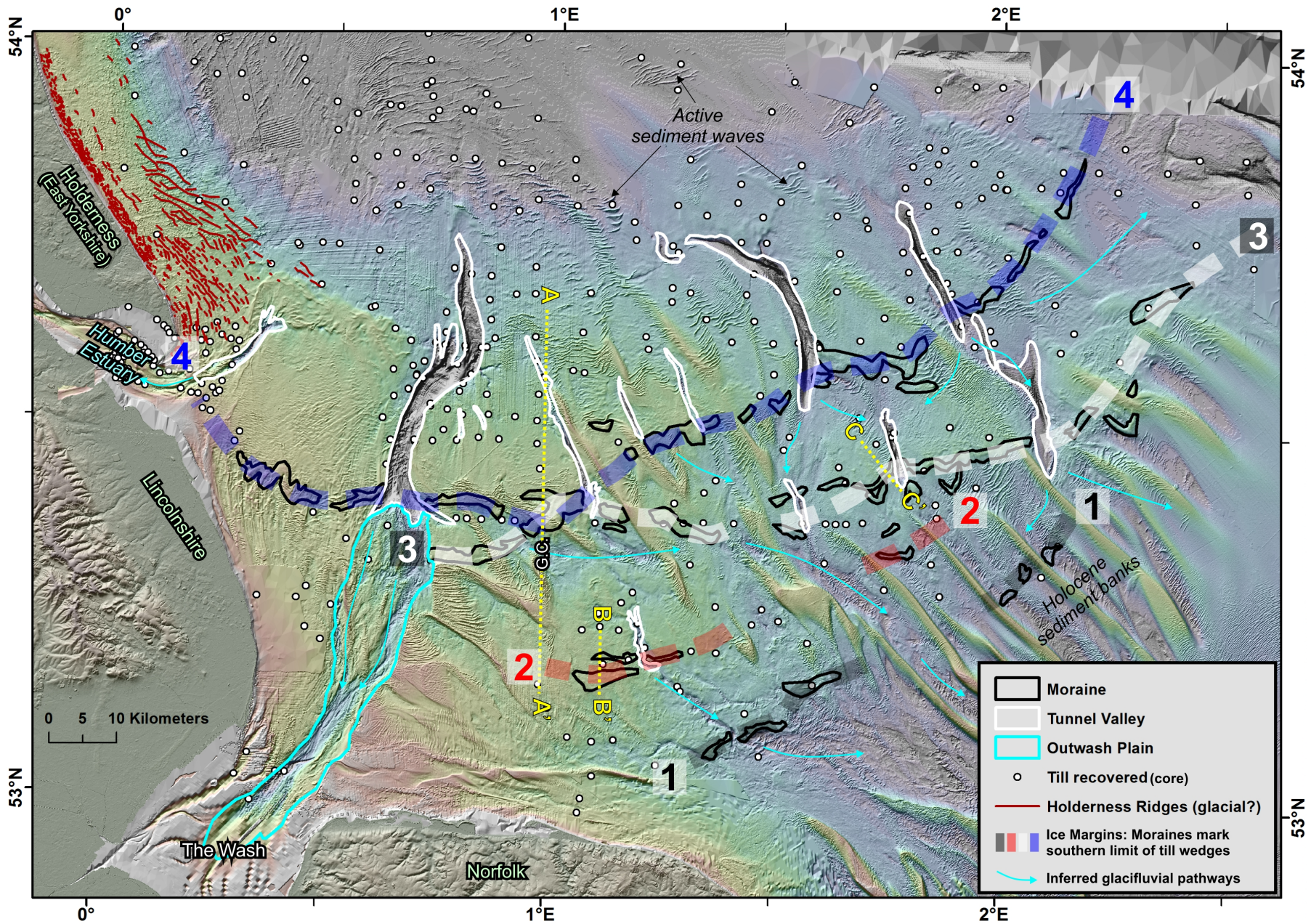


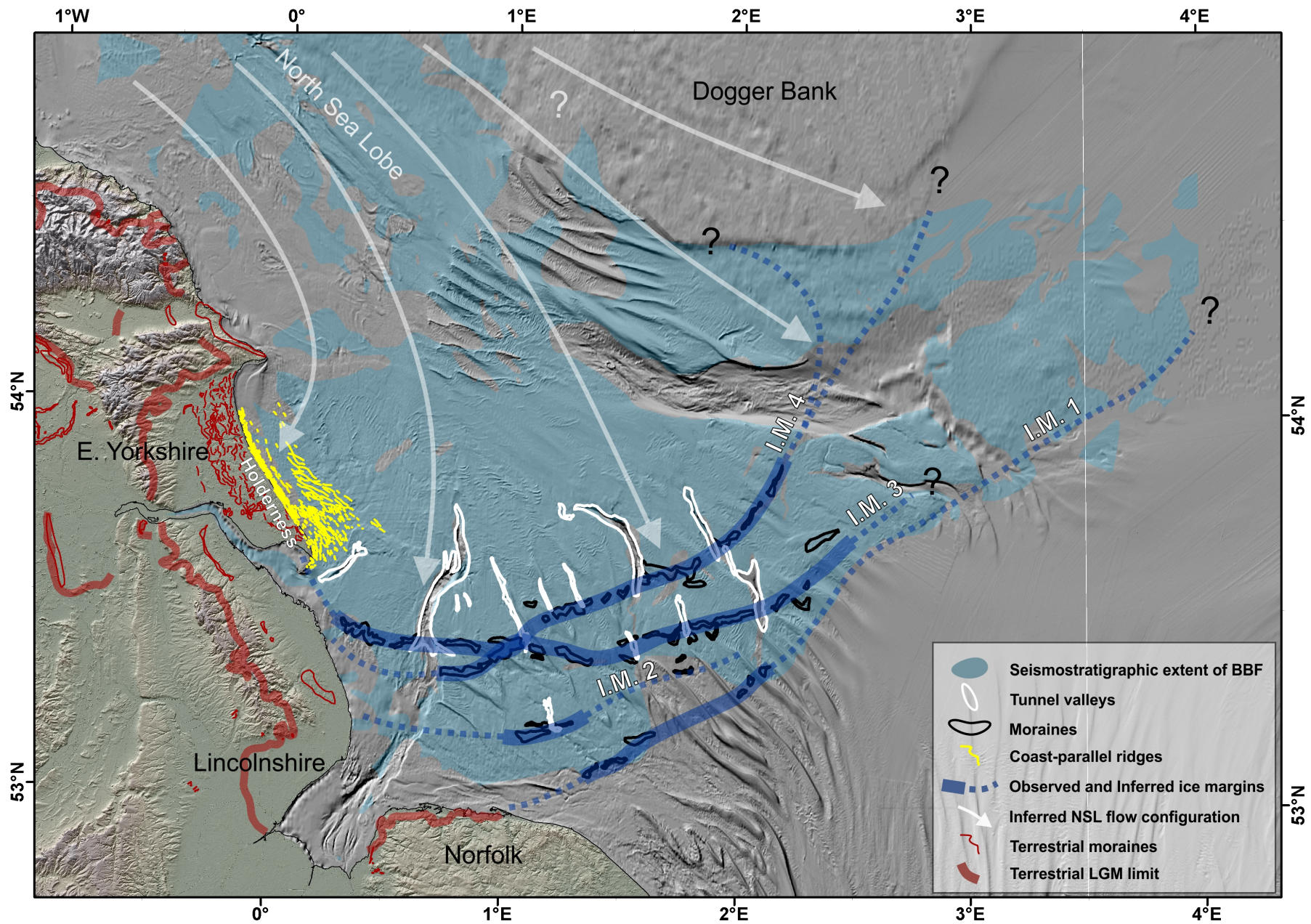
B'-----B

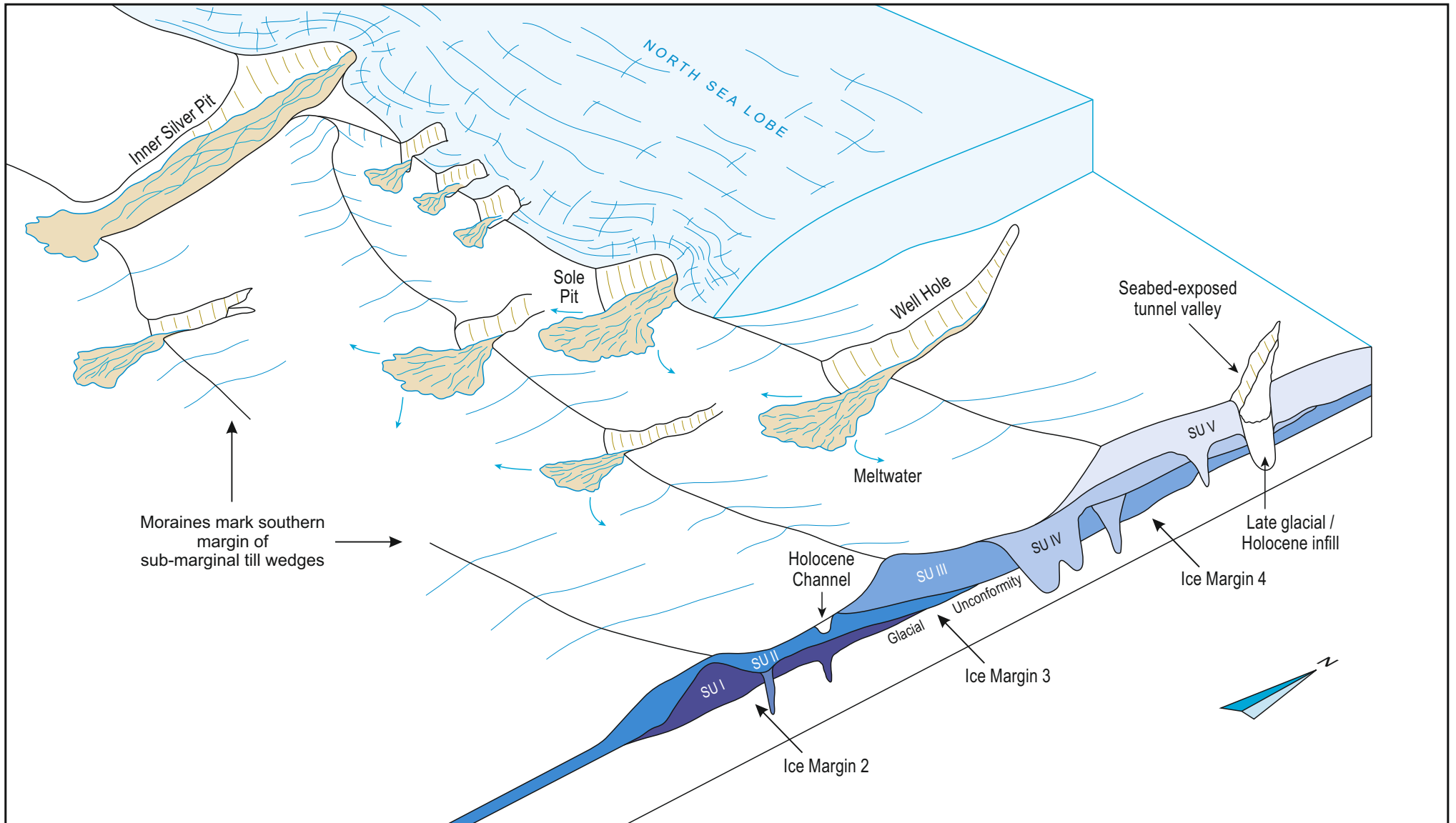


C'-----C



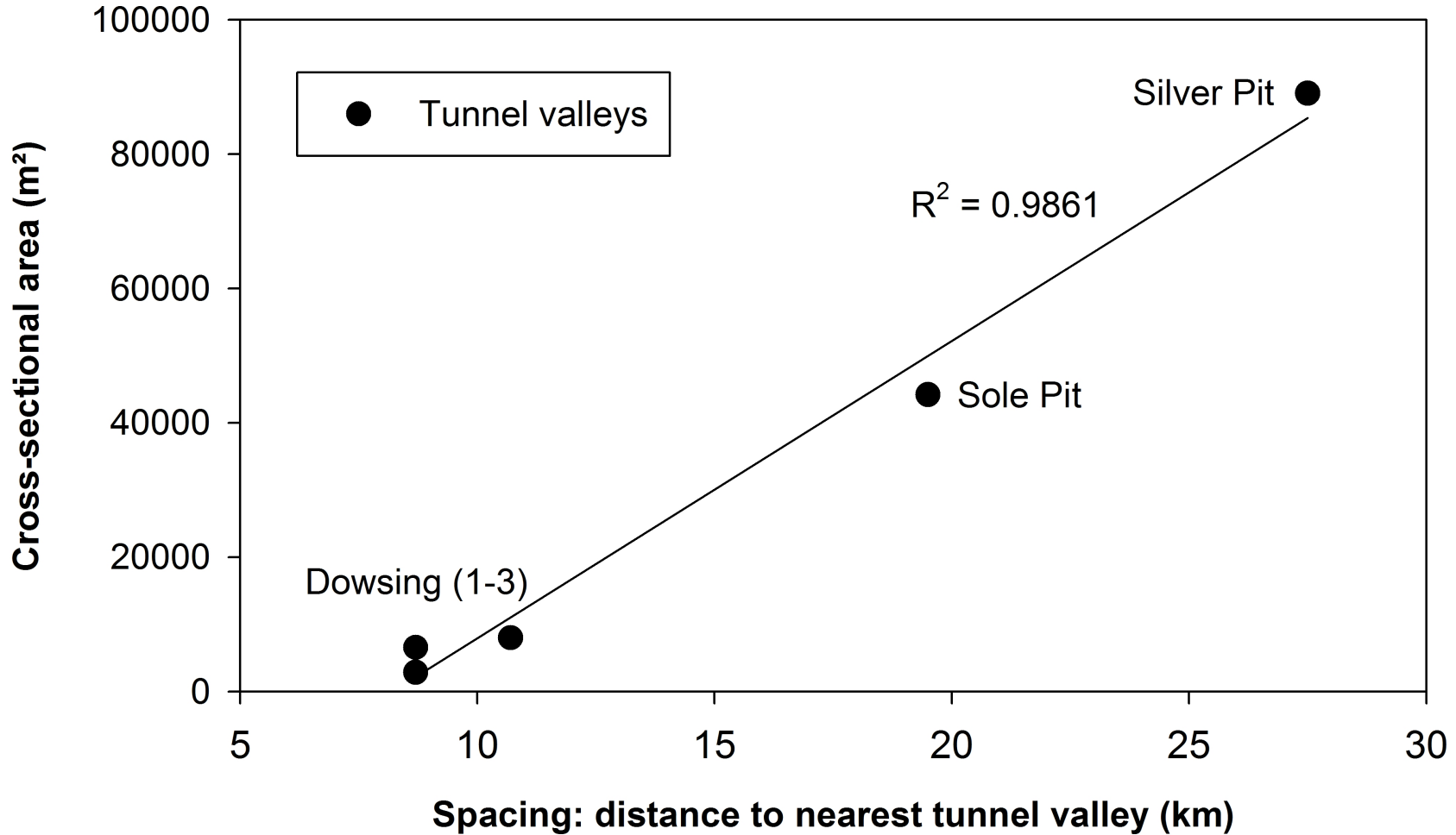






**Tunnel Valley (Spacing vs. Drainage)**

	Silver Pit	Dowsing-1	Dowsing-2	Dowsing-3	Sole Pit
Spacing (nearest valley) (km)	27.5	10.7	8.7	8.7	19.5
Cross-sectional area (m <sup>2</sup> )	89054.0	8010.1	6577.0	2855.0	44179.4



## Highlights for Manuscript:

“Phased occupation and retreat of the last British–Irish Ice Sheet in the southern North Sea; geomorphic and seismostratigraphic evidence of a dynamic ice lobe”

- Detailed reconstruction of MIS 2 glaciation in S. North Sea based on marine data;
- Extensive bathymetry data reveal terminal positions of former North Sea Lobe (NSL);
- Seabed landforms relate to previously undetected seismostrat. architecture;
- Landform/subsurface assemblage constrains relative chronology, fits onshore record;
- Tunnel valley origin linked to discrete ice margins; size proportional to catchment.